Published for SISSA by Springer

Received: *January 21, 2024*
Revised: *August 31, 2024*
Accepted: *December 13, 2024*
Published: *January 2, 2025*

Measurement of the double-differential inclusive jet cross section in proton-proton collisions at $\sqrt{s} = 5.02$ TeV

The CMS collaboration

E-mail: cms-publication-committee-chair@cern.ch

Abstract: The inclusive jet cross section is measured as a function of jet transverse momentum p_{T} and rapidity y. The measurement is performed using proton-proton collision data at $\sqrt{s} = 5.02$ TeV, recorded by the CMS experiment at the LHC, corresponding to an integrated luminosity of $27.4\,\mathrm{pb}^{-1}$. The jets are reconstructed with the anti-k_{T} algorithm using a distance parameter of $R = 0.4$, within the rapidity interval $|y| < 2$, and across the kinematic range $0.06 < p_{\mathrm{T}} < 1$ TeV. The jet cross section is unfolded from detector to particle level using the determined jet response and resolution. The results are compared to predictions of perturbative quantum chromodynamics, calculated at both next-to-leading order and next-to-next-to-leading order. The predictions are corrected for nonperturbative effects, and presented for a variety of parton distribution functions and choices of the renormalization/factorization scales and the strong coupling α_{S}.

Keywords: Hadron-Hadron Scattering, Jet Physics, QCD

ArXiv ePrint: 2401.11355

https://doi.org/10.1007/JHEP01(2025)011

JHEP01(2025)011

Contents

1 Introduction

One of the most fundamental standard model (SM) measurements is that of the production cross section of jets in hadron collisions. When performed double-differentially, as a function of both transverse momentum (p_{T}) and rapidity (y) of the produced jets, it provides an opportunity to thoroughly study the jet kinematics. In the inclusive jet production, almost all of the jets are initiated from pure quantum chromodynamics (QCD) processes, with negligible background coming from intermediate electroweak processes with jet final states. This allows for a direct comparison of experimental results with perturbative QCD (pQCD) calculations corrected for the nonperturbative (NP) effects of hadronization and multiparton interactions. Since the final measured hadronic cross section may be described as a convolution of the partonic cross section with parton distribution functions (PDFs) of the initial-state hadrons, the measurement offers constraints on PDFs and the strong coupling (α_{S}), as well as a better

JHEP01(2025)011

understanding of the factorization and renormalization scales. It is also important to perform the measurement at different values of the center-of-mass energy ($\sqrt{s}$) of the colliding hadrons, because this affects the energy scales and strength of the interactions. In this paper, we present the measurement of the double-differential cross section of inclusive jet production in proton-proton (pp) collisions at $\sqrt{s} = 5.02\,\text{TeV}$ with an integrated luminosity of $27.4\,\text{pb}^{-1}$. The measurement is performed with data collected in 2015 by the CMS experiment during a special lower-energy run of the Large Hadron Collider (LHC) at CERN.

Measurements of the inclusive jet cross section have been performed: in pp collisions at the CERN Intersecting Storage Rings (ISR) at $\sqrt{s}$ equal to 45 GeV [1], and 63 GeV [2]; in proton-antiproton collisions at the CERN Super Proton Antiproton Synchrotron (Sp$\bar{\text{p}}$S) at 540–546 GeV [3, 4], 630 GeV [5, 6], and 200–900 GeV [7]; in proton-antiproton collisions at the Fermilab Tevatron at 546 GeV [8], 630 GeV [9, 10], 1.8 TeV [11, 12], and 1.96 TeV [13–17]; and in pp collisions at the LHC at 2.76 TeV [18–20], 7 TeV [21–27], 8 TeV [28, 29], and 13 TeV [30–33]. All these measurements led to a better understanding of pQCD within the constraints of NP QCD effects. At the same time, they provided accurate estimations of QCD-initiated backgrounds in both SM analyses and direct searches for new physics, and offered the possibility of indirect discoveries.

The presented cross section measurement has the added value of providing a reference for the respective 5.02 TeV heavy-ion jet analyses probing the quark-gluon plasma [34–38]. In such plasma conditions, because of jet quenching [39], the resulting jets demonstrate differences in the parton showering [40], fragmentation [41], and momentum imbalance in back-to-back dijets [42, 43], compared with the respective jets produced in pp collisions.

The paper is structured as follows. In section 2, we present the cross section measurement strategy and in section 3 we give a brief description of the CMS experiment. The jet reconstruction, identification, and resolution are described in section 4, and in section 5 we present the online data collection and trigger efficiencies. The simulation and detector-level spectra are discussed in sections 6 and 7, respectively. In section 8, the pQCD prediction and the estimation of the NP effects are given. In section 9, we discuss the procedure of unfolding the detector-level spectra to particle-level. The experimental and theoretical systematic uncertainties are detailed in section 10. The final experimental results and the comparisons with theoretical predictions are shown in section 11, and a summary is given in section 12. Tabulated results are provided in the HEPData record for this analysis [44].

2 The double-differential inclusive jet cross section

The inclusive jet cross section, differential in jet p_T and y, is defined as:

$$\frac{\mathrm{d}^2\sigma}{\mathrm{d}p_\mathrm{T}\mathrm{d}y} = \frac{N_\text{jets}}{\epsilon\mathcal{L}\Delta p_\mathrm{T}\Delta y}, \tag{2.1}$$

where N_jets is the number of jets observed within the bins of p_T and y (that have widths Δp_T and Δy, respectively), $\mathcal{L}$ is the integrated luminosity of the data set, and ϵ is the product of the event selection, jet selection, and trigger efficiencies. In this measurement, the bin width Δp_T varies with p_T according to the momentum resolution of the detector and the size of the available data sample. The range of y in this analysis is $|y| < 2$, and the cross section is measured in four bins of $|y|$, each with width of $\Delta|y| = 0.5$ (thus $\Delta y = 1$).

Equation (1) can be applied in a straightforward manner to the detector-level jet cross section, where jets are reconstructed from detected particles and are counted in bins of p_{T} vs. $|y|$. On the other hand, the desirable quantity to be measured is the particle-level jet cross section, where jets are reconstructed from stable particles (with mean path length $c\tau > 10\,\mathrm{mm}$), not affected by detector effects. This is achieved by correcting the detector-level jet count in each p_{T} bin for bin migrations due to the limited detector momentum resolution (migrations in $|y|$ are negligible). The transition from detector-level to particle-level jet cross section is achieved with an unfolding procedure. The particle-level cross section measurement is the final result, to be compared with theoretical predictions.

3 The CMS experiment

The CMS experiment uses a right-handed coordinate system, with the origin at the nominal interaction point, the x axis pointing to the center of the LHC ring and the z axis along the counterclockwise-beam direction as viewed from above. The polar angle θ is measured from the positive z axis and the azimuthal angle ϕ is measured on the x-y plane. The pseudorapidity η is defined as $-\ln(\tan(\theta/2))$.

The central feature of the CMS apparatus is a superconducting solenoid of 6 m internal diameter, providing a magnetic field of 3.8 T. Within the magnetic volume are a silicon pixel and strip tracker, a lead tungstate crystal electromagnetic calorimeter (ECAL), and a brass and scintillator hadron calorimeter (HCAL), each composed of a barrel and two endcap sections. Forward calorimeters extend the η coverage provided by the barrel and endcap detectors. Muons are detected in gas-ionization chambers embedded in the steel flux-return yoke outside the solenoid.

The ECAL consists of 75848 lead tungstate crystals, which provide coverage in $|\eta| < 1.48$ in the barrel region and $1.48 < |\eta| < 3.00$ in two endcap regions. Preshower detectors consisting of two planes of silicon sensors interleaved with a total of 3 radiation lengths of lead are located in front of each ECAL endcap detector.

In the region $|\eta| < 1.74$, the HCAL cells have widths of 0.087 in both $|\eta|$ and ϕ in radians. In the η-ϕ plane, and for $|\eta| < 1.48$, the HCAL cells map onto $5{\times}5$ arrays of ECAL crystals to form calorimeter towers projecting radially outwards from close to the nominal interaction point. For $|\eta| > 1.74$, the coverage of the towers increases progressively to a maximum of 0.174 in $\Delta\eta$ and $\Delta\phi$ in radians. Within each tower, the energy deposits in ECAL and HCAL cells are summed to define the calorimeter tower energies, which are subsequently used to provide the energies and directions of hadronic jets. When combining information from the entire detector, the jet energy resolution amounts typically to 15–20% at 30 GeV, 10% at 100 GeV, and 5% at 1 TeV [45].

Events that are considered potentially interesting are selected online by a two-tiered trigger system [46]. The first level (L1), composed of custom hardware processors, uses information from the calorimeters and muon detectors to select events at a rate of around 100 kHz within a fixed latency of about 4 μs [47]. The second level, known as the high-level trigger (HLT) [48], consists of a farm of processors running a version of the full event reconstruction software optimized for fast processing, and reduces the event rate to around 1 kHz before data storage. A more detailed description of the CMS detector can be found in ref. [49].

4 Jet reconstruction, identification, and resolution

Final-state particles are reconstructed using the particle-flow (PF) algorithm [50], which combines signals from all CMS subdetectors. The energy of the particles is obtained as follows:

- for photons, from the ECAL measurement;
- for electrons, from a combination of the electron momentum at the primary interaction vertex as determined by the tracker, the energy of the corresponding ECAL cluster, and the energy sum of all bremsstrahlung photons compatible in space and time with originating from the electron track;
- for muons, from the curvature of the corresponding track measured in both the tracker and the muon system;
- for charged hadrons, from a combination of their momentum measured in the tracker and the matching ECAL and HCAL energy deposits. This energy is corrected for the response function of the calorimeters to hadronic showers;
- for neutral hadrons, from the corresponding corrected ECAL and HCAL energies.

These particles are used as constituents in the anti-k_T jet reconstruction algorithm [51], implemented in FastJet [52], with a distance parameter $R = 0.4$. Charged hadrons originating from vertices other than the primary vertex (PV) are removed to reduce effects from multiple interactions per proton bunch crossing of the colliding beams (pileup). The PV is required to be reconstructed from at least five charged-particle tracks and must satisfy a set of quality requirements, including $|z_{PV}| < 24$ cm and $\rho_{PV} < 2$ cm, where z_{PV} and ρ_{PV} are the longitudinal and transverse distances of the PV from the nominal interaction point in the CMS detector. In the case that multiple vertices pass these requirements, the PV is taken to be the vertex corresponding to the hardest scattering in the event, evaluated using tracking information alone, as described in section 9.4.1 of ref. [53].

In order to reduce the probability of misidentification, the jets used in this analysis are required to satisfy the following quality requirements. Jets are required to have at least two PF-constituents, with at least one being charged. The fractions of neutral hadron energy, neutral electromagnetic energy, and charged electromagnetic energy of the jets each must not exceed 99% of the jet's total energy. The muon energy fraction is required to be less than 80% of this total energy and the charged-hadron energy must be nonzero.

The jet momenta used in the above fractions are the raw jet momenta, determined as the vectorial sum of all constituents' particle momenta. Because of calorimeter nonlinearities, pileup effects, and excess energy from the underlying event, the raw measured energy of the jets is corrected in a factorized approach using dedicated data samples and Monte Carlo (MC) simulations. There are two levels of corrections for jets both in MC simulation and data: a correction for pileup and electronic noise; and a correction for the response of the detector as a function of jet p_T and η. An additional residual correction is applied only to jets in data, to account for differences between data and MC [54]. These jet energy scale corrections (JES) are derived from simulation studies so that the average measured energy of jets becomes identical to that of particle-level jets. In situ measurements of the momentum balance in dijet, photon+jet, Z +jet, and multijet events are used to determine any residual differences between the jet energy scale in data and in simulation, and appropriate corrections are made [45]. The corrected energy is used in the measured and simulated jet p_T distributions presented.

An important aspect of this analysis is the determination of the jet energy resolution (JER) as a function of jet p_T and y. The JER provides the correlation between particle-level jet energy and the corresponding detector-level one, needed for unfolding the results to particle level. The JER is determined by first creating the ratios of detector-level jet p_T over the corresponding particle-level value, p_T^{det}/p_T^{part}, using simulation, in bins of p_T^{part} and rapidity. The cores of these distributions are fitted with Gaussian distributions with varied normalization, mean (μ_G) and standard-deviation (σ_G) values. These JER Gaussian functions are used for spreading the jet p_T generated via pseudo-experiments during the construction of the response matrices. In order to achieve a smoother unfolding, the μ_G and σ_G distributions as a function of p_T are fitted with continuous curves, in each rapidity bin separately, so that a more accurate spreading is achieved for each pseudo-experiment-generated p_T. A more complicated approach, which uses double-sided Crystal Ball functions with the addition of extra tails in order to describe the detector effects, was also implemented, with consistent unfolded results. The simpler Gaussian method is preferred since it provides smoother unfolded results, because of the fits of the μ_G and σ_G p_T distributions. The extracted JER values (σ_G) are corrected with a scale factor of 1.1 ± 0.1, in order to account for the differences in jet p_T resolution between data and MC simulation, as was done in ref. [37]. The 10% systematic uncertainty in JER is derived from the variation of the spreading of jet p_T in the MC dijet spectrum so that the latter matches the observed one in the data. The estimation of the resolution in the data is obtained by comparing the p_T of the leading two jets in events with low extra jet activity.

5 Data collection and trigger efficiencies

We analyze data collected during a special LHC pp run at $\sqrt{s} = 5.02\,\text{TeV}$, characterized by low instantaneous luminosity that resulted in an average 1.1 collisions per bunch crossing with a reconstructed primary vertex. The corresponding integrated luminosity of the data set is $27.4\,\text{pb}^{-1}$.

The HLT selection consists of three separate single-jet trigger paths, designated here as ak4PFjet{40,60,80}. The three triggers each require at least one jet in the event (reconstructed at HLT level) with transverse momentum p_T^{HLT} larger than 40, 60, and 80 GeV, respectively. The respective thresholds at L1 level were 28, 40, and 48 GeV. The 40 and 60 GeV triggers are prescaled, i.e., their data output rate is algorithmically reduced to accommodate the allocated bandwidth. This means that the jet yields from those triggers have to be scaled up to account for the full integrated luminosity. In order to remove trigger-efficiency dependence on the measured jet rates, we utilize triggers for jet p_T above a threshold where they are fully efficient (efficiency >99.9%). We measure each trigger efficiency as a function of the triggered

JHEP01(2025)011

jet p_T using a tag-and-probe method applied on the same mutlijet data. In this method, we tag a jet that passed the trigger in question, we remove it, and we use the remaining (probe) jets to form a jet-p_T-dependent ratio (trigger efficiency) of number of jets that pass the trigger divided by the number of jets that pass some looser requirements (e.g., L1 trigger or a lower-p_T trigger). We conclude that the ak4PFjet{40,60,80} triggers are fully efficient for jet p_T above 55, 75, and 105 GeV, respectively. The proper merging of the data collected from these three triggers gives the detector-level jet spectra presented in section 7.

We select for further processing events that are not associated with noise, which could come from either the calorimeters or beam halo effects. We achieve this by requiring that the ratio of the momentum imbalance in the transverse plane to the scalar sum of the PF constituents' transverse momentum is less than 0.3, as required also in refs. [20, 24, 28]. This selection requirement also suppresses jets associated with the production and decay of electroweak gauge bosons and top quarks. The final data set includes events with the presence of a PV and with at least one jet passing the identification requirements presented in section 4.

6 Monte Carlo simulation

Monte Carlo techniques are used to simulate events in the CMS detector, as well as for verifications and corrections. PYTHIA 8 [55] generates jets with $2 \to 2$ leading-order (LO) Feynman diagrams, p_T-ordered dipole showering of outgoing partons, and subsequent hadronization using the Lund string model [56]. The NNPDF2.3 [57] LO PDF set is used along with the Monash [58]-based CUETP8M1 underlying event tune [59] for PYTHIA 8, which uses CMS minimum bias data to describe the underlying event. HERWIG 7 [60] is used at LO $2 \to 2$ mode. The NNPDF3.1 [61] next-to-next-to-LO (NNLO) PDF set with $\alpha_S(m_Z) = 0.118$ is used (where m_Z is the pole mass of the Z boson), and the NNPDF3.1 LO PDF set is used for the determination of multiparton interactions. Angular-ordered showers are hadronized based on the cluster model [62]. The CH2 tune [63] is used for the description of the underlying event. The events produced by the above generators pass through a GEANT4 [64]-based CMS detector simulation giving signals that are used for the final reconstructed detector-level objects.

The PYTHIA 8 simulation, version 212, is used for an initial comparison of the spectra measured in data and simulation at the detector level (section 7), and for the determination of the JER (section 4). The PYTHIA 8 simulation, version 219, is used for the estimation of the NP corrections to the pQCD calculation (section 8). The HERWIG 7 simulation, version 2.0, is used for an alternate estimation of the NP effects.

7 Detector-level spectra

The inclusive detector-level jet p_T spectra, constructed from data collected with the three single-jet HLT paths, have to be merged so that the resulting spectra correspond to the true respective jet p_T distributions, without any effects from trigger inefficiencies or trigger prescales, and without any double-counting of events or jets.

In this analysis, we create three separate detector-level jet spectra, using data from each trigger as a separate experiment with its own integrated luminosity, which is determined by integrating the instantaneous luminosity with the corresponding event-by-event prescales.

In the separate spectra from the ak4PFjet{40,60,80} triggers, jets with p_T above 55, 75, 105 GeV, respectively, are included. Subsequently, the three spectra are merged, by keeping only the jets from the three spectra that belong in the three full-efficiency p_T windows, $56 < p_\mathrm{T} < 75\,\mathrm{GeV}$, $75 < p_\mathrm{T} < 105\,\mathrm{GeV}$, and $p_\mathrm{T} > 105\,\mathrm{GeV}$, respectively. The spectra are divided by their luminosities, to provide the detector-level cross sections, as shown below:

$$\frac{\mathrm{d}^2\sigma^{\mathrm{det}}}{\mathrm{d}p_\mathrm{T}\mathrm{d}y} = \frac{1}{\epsilon\Delta p_\mathrm{T}\Delta y}\begin{cases}\frac{N_{\mathrm{jets}}^{\mathrm{jet40}}}{\mathcal{L}^{\mathrm{jet40}}} & \text{if } 56 < p_\mathrm{T} < 75\,\mathrm{GeV}\\ \frac{N_{\mathrm{jets}}^{\mathrm{jet60}}}{\mathcal{L}^{\mathrm{jet60}}} & \text{if } 75 < p_\mathrm{T} < 105\,\mathrm{GeV}\\ \frac{N_{\mathrm{jets}}^{\mathrm{jet80}}}{\mathcal{L}^{\mathrm{jet80}}} & \text{if } p_\mathrm{T} > 105\,\mathrm{GeV}\end{cases} \tag{7.1}$$

where $N_{\mathrm{jets}}^{\mathrm{jet\{40,60,80\}}}$ are the numbers of accepted jets recorded by the ak4PFjet{40,60,80} triggers, and $\mathcal{L}^{\mathrm{jet\{40,60,80\}}}$ are their luminosities, 0.96, 4.4, and $27.4\,\mathrm{pb}^{-1}$, respectively. Now, the total efficiency ϵ is consistent with unity, given the use of the full-efficiency p_T windows. The merging and the resulting detector-level cross section, differential in p_T, are shown in figure 1.

The detector-level measured inclusive jet cross sections, separately for each of the four rapidity bins, can be seen in figure 2. Overlaid is the PYTHIA 8 distribution, normalized to the respective detector event yields for shape comparison. Being an LO generator, PYTHIA 8 is not expected to fully describe the absolute yields and shapes of the observed measured spectra. Nevertheless, there is a good agreement between the PYTHIA 8 prediction and the observed data in the shape of the detector-level p_T distribution of the cross section in all $|y|$ bins, over several orders of cross section magnitude, as the ratios between data and simulation of figure 2 show. For an appropriate comparison with the SM predictions, the detector-level spectra need to be corrected to the particle-level spectra through the unfolding procedure (section 9). The comparisons will be performed against the fixed-order pQCD predictions, corrected for the NP effects presented in the next section.

8 Perturbative QCD predictions and estimation of NP effects

The next-to-LO (NLO) pQCD prediction for the inclusive jet cross section at 5.02 TeV is determined using the NLOJET++ program [65, 66] (version 4.1.3), whereas the NNLO pQCD prediction is determined with the NNLOJET [67–70] package (revision 5918), both run within the FASTNLO framework [71] (version 2.5). The prediction depends on the PDF set used as well as the choice of renormalization scale (μ_R) and factorization scale (μ_F). In this paper, we present the NLO (NNLO) perturbative predictions for the CT18NLO [72] (CT18NNLO [72], NNPDF3.1NNLO [61]) PDF sets, accessible through the LHAPDF6 package [73]. The predictions are computed using one of two scale options: either $\mu = \mu_\mathrm{R} = \mu_\mathrm{F} = H_\mathrm{T}$, where H_T is the scalar sum of the p_T values of all partons in each event (an event-based quantity), or $\mu = \mu_\mathrm{R} = \mu_\mathrm{F} = p_\mathrm{T}$, where p_T is that of each jet in the event (a jet-based quantity). All fixed-order pQCD predictions are binned in jet p_T and are subsequently interpolated with a cubic spline, which allows for a more accurate application of the NP corrections and the subsequent rebinning of the cross section distributions through integration.

This pQCD prediction has to be corrected for the NP effects of multiparton interactions and hadronization, which are estimated using both PYTHIA 8 and HERWIG 7. This estimation

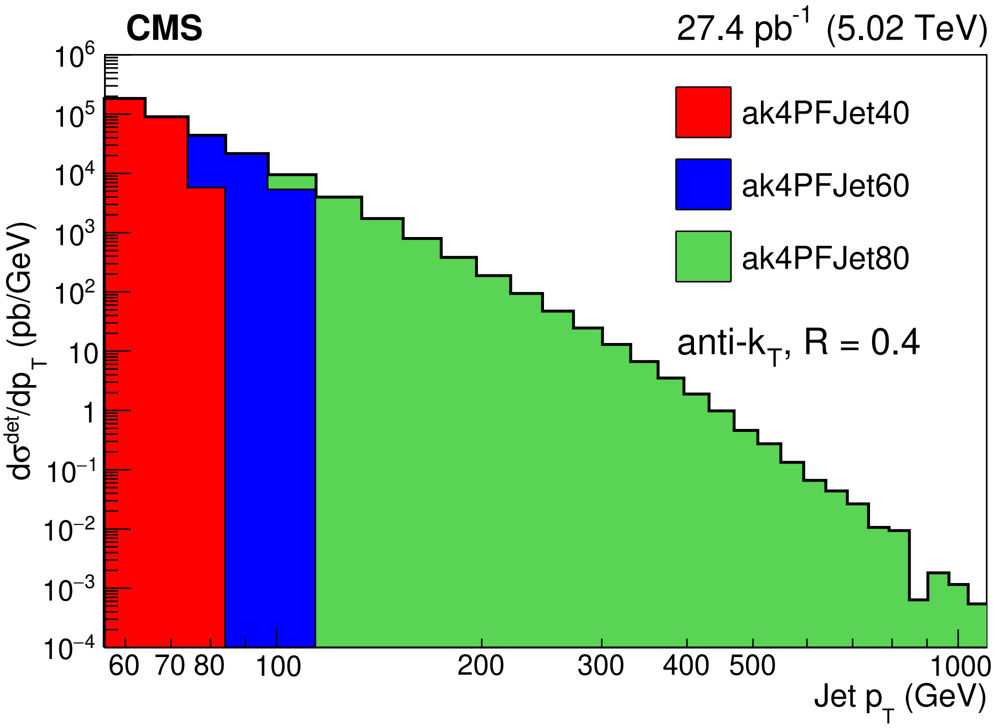

Figure 1. Detector-level cross section obtained after merging the contributions from the three triggers, normalized to their respective integrated luminosities.

is achieved by running the generators with and without the NP effects and dividing the corresponding spectra. These runs do not include the detector simulation. Because the hadronization and multiparton interaction modeling of the two generators differ, we do not expect them to predict the same NP effects. Indeed, the HERWIG 7-derived corrections are larger than those of PYTHIA 8. In this analysis, we correct the perturbative spectra by multiplying them with the average of the two corrections and we use half the difference as a systematic uncertainty. Figure 3 shows the NP correction as a function of jet p_T, for $|y| < 0.5$, along with the systematic uncertainty. Similar distributions are extracted for all rapidity bins.

9 Unfolding measurement to particle-level spectra

The unfolding method used in this analysis is based on the least-squares minimization, implemented with the TUNFOLD [74] package in each rapidity window. The quantity that is minimized is

$$L = (\mathbf{u} - \mathbf{A}\mathbf{x})^{\intercal}\mathbf{V}^{-1}(\mathbf{u} - \mathbf{A}\mathbf{x}), \tag{9.1}$$

where $\mathbf{u}$ is the vector of the observed detector-level spectrum (with dimension equal to the number of bins at detector level), with background removed as described later, $\mathbf{x}$ is the vector of the unfolded particle-level spectrum (with dimension equal to the number of bins at unfolded level), $\mathbf{A}$ is the probability matrix, and $\mathbf{V}$ is the data covariance matrix. The probability matrix is the result of row-wise normalization of the response matrix (described below) so that each 2D bin content equals the probability that a jet in that particle-level p_T

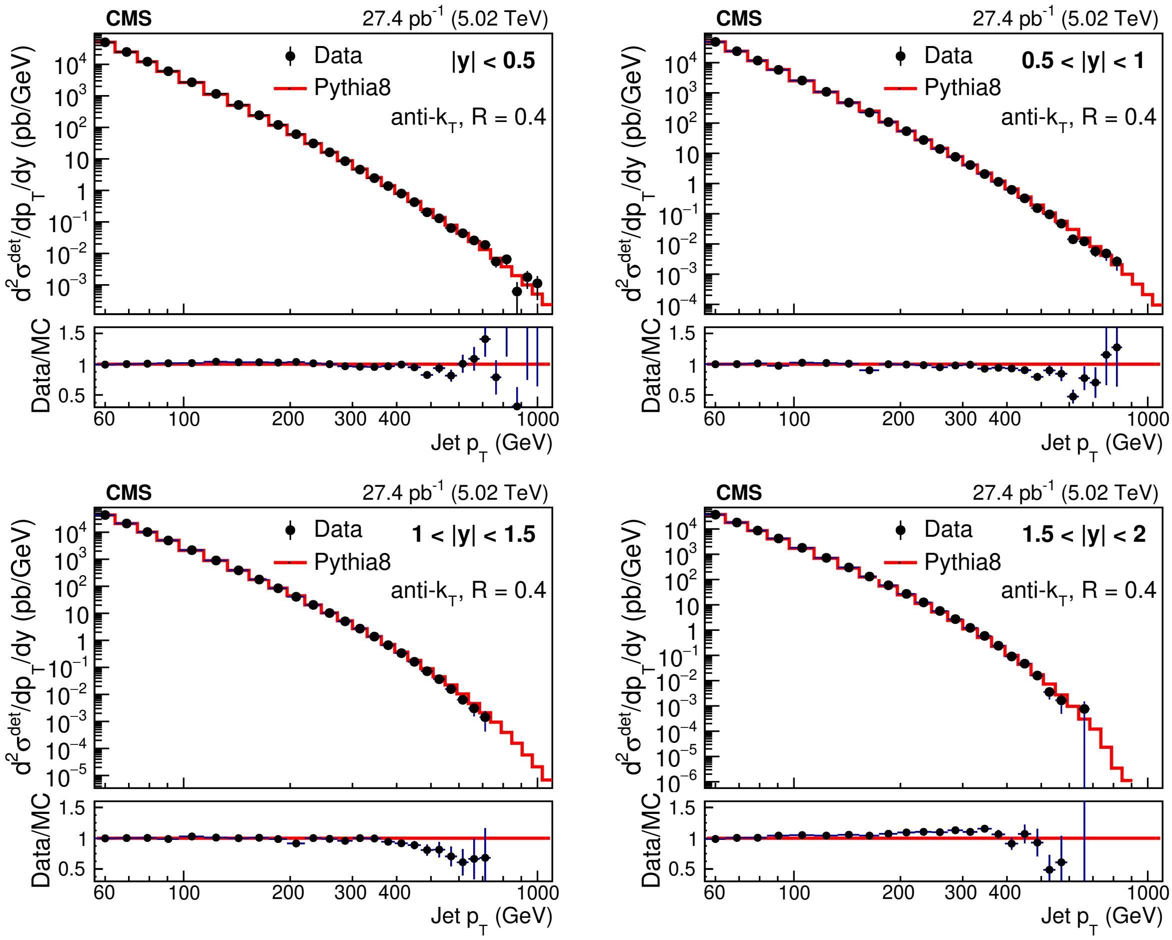

Figure 2. Detector-level inclusive jet cross section, differential in p_{T}, for the four rapidity bins, for the data (points) and the PYTHIA 8 prediction (line) normalized to the total cross section of the data. The lower panels show the ratio of the two distributions. The error bars show the statistical uncertainties in the data.

bin is detected in the respective detector-level p_{T} bin. The inverse of the data covariance matrix is included to take into account the differing accuracy of the elements of the data vector. No explicit regularization or area constraint is used because they could bias the results. As a form of implicit regularization, the particle-level binning is coarser than the detector-level binning. This helps to moderate the effect of bin migrations and detector-level statistical fluctuations that can cause unphysical behavior in the unfolded result. The detector-level and particle-level p_{T} binning for each $|y|$ bin is shown in table 1.

The covariance matrices are necessary to properly determine the statistical uncertainty of the measurement where multiple jets can be detected per collision event. If $\mathbf{q}$ is the column vector resulting from the one-dimensional histogram of measured detector-level jet p_{T} for an event, then the sum of the outer products $\mathbf{q}\times\mathbf{q}^{\mathrm{T}}$ for all detected events constructs a numerical approximation of the two-dimensional covariance matrix. Figure 4 shows the covariance matrices for the four rapidity bins. In the unfolding, the entire matrices are used, whereas in

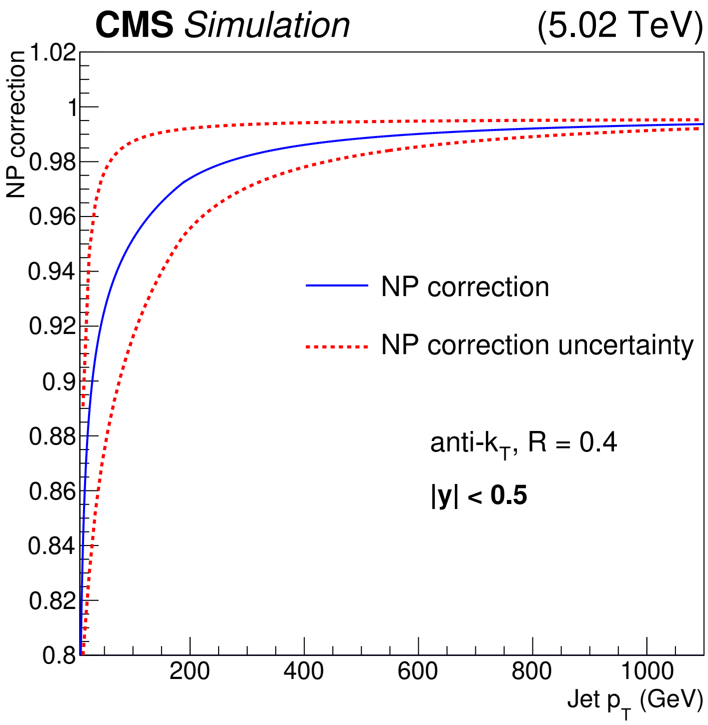

Figure 3. Nonperturbative correction to the fixed-order QCD calculation of inclusive jet cross section, as a function of jet p_{T}, for the $|y| < 0.5$ rapidity bin. Dashed lines show the prediction of corrections using HERWIG 7 (lower line) and PYTHIA 8 (upper line). The central solid line shows the average NP correction used in this analysis, with an uncertainty defined by the extreme predictions. The NP corrections are similar in shape and value for the other rapidity bins.

	$\|y\|$ binning	p_{T} binning (GeV)
detector-level spectra	all rapidities	{56, 64, 74, 84, 97, 114, 133, 153, 174, 196, 220, 245, 272, 300, 330, 362, 395, 430, 468, 507, 548, 592, 638, 686, 737, 790, 846, 905, 967, 1032, 1101}
particle-level spectra	0.0–0.5	{64, 84, 114, 153, 196, 245, 300, 395, 507, 638, 846}
	0.5–1.0	{64, 84, 114, 153, 196, 245, 300, 395, 507, 638, 846}
	1.0–1.5	{64, 84, 114, 153, 196, 245, 330, 395, 507, 638 }
	1.5–2.0	{64, 84, 114, 153, 196, 245, 330, 395, 507}

Table 1. The edges of the p_{T} bins for the detector-level spectra (all rapidities) and for the particle-level spectra (per rapidity bin).

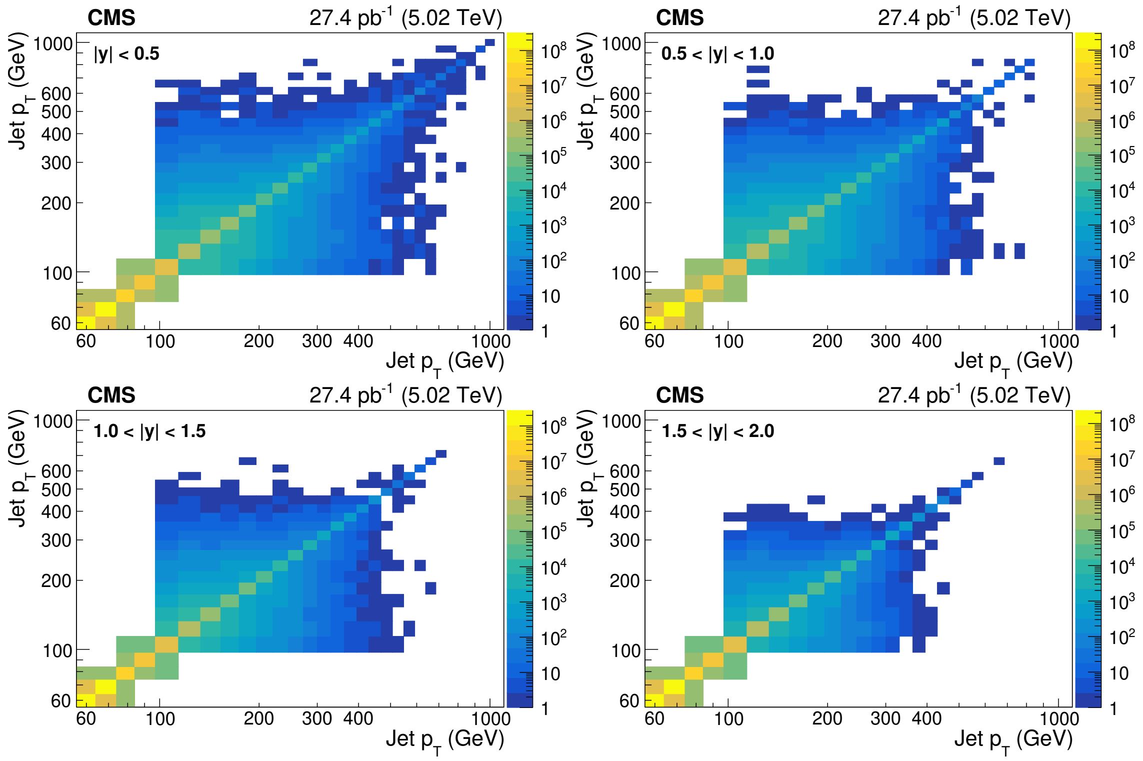

Figure 4. The covariance matrices of the observed detector-level jet p_{T} for the four rapidity bins. The color scale reports the product of the effective number of jets in the respective p_{T} bin combinations.

the presentation of detector-level spectra (as in figure 2), the square roots of the diagonal elements of the covariance matrices are used to present the statistical uncertainty.

The response matrix is a two-dimensional histogram filled with the ($p_{\mathrm{T}}^{\mathrm{det}}$,$p_{\mathrm{T}}^{\mathrm{part}}$) pairs of detector-level jet p_{T} and its corresponding particle-level jet p_{T}. In this analysis we fill this histogram using pseudo-experiments, where we generate random p_{T} values using the expected smooth theoretical spectra (smooth NLO splines multiplied by smooth NP corrections, shown in figure 3 for $|y| < 0.5$), to obtain $p_{\mathrm{T}}^{\mathrm{part}}$, and subsequently smear them using the JER, to obtain the corresponding $p_{\mathrm{T}}^{\mathrm{det}}$.

Figure 5 shows the response matrices for the four rapidity bins. The range of the detector- and particle-level axes corresponds to the detector-level binning and particle-level binning, respectively. During the filling of the response matrices, we naturally have $p_{\mathrm{T}}^{\mathrm{part}}$ values within the particle-level range that give $p_{\mathrm{T}}^{\mathrm{det}}$ outside the detector-level range. The fraction of these jets gives an estimate of the number of the jets missed due to the finite detector resolution. At the same time, some $p_{\mathrm{T}}^{\mathrm{part}}$ values that are outside the particle-level range correspond to $p_{\mathrm{T}}^{\mathrm{det}}$ values within range. The fraction of these jets provides an estimate of background, i.e., jets that migrated to the measured spectrum from a different particle-level jet kinematic region. We select the particle-level binning to start at a higher p_{T} value than the detector-level binning (64 vs. 56 GeV) in order to reduce the amount of missed jets (they become less than 0.1% of the jet content of the first p_{T} bin of the unfolded spectrum and practically zero after the third bin).

JHEP01(2025)011

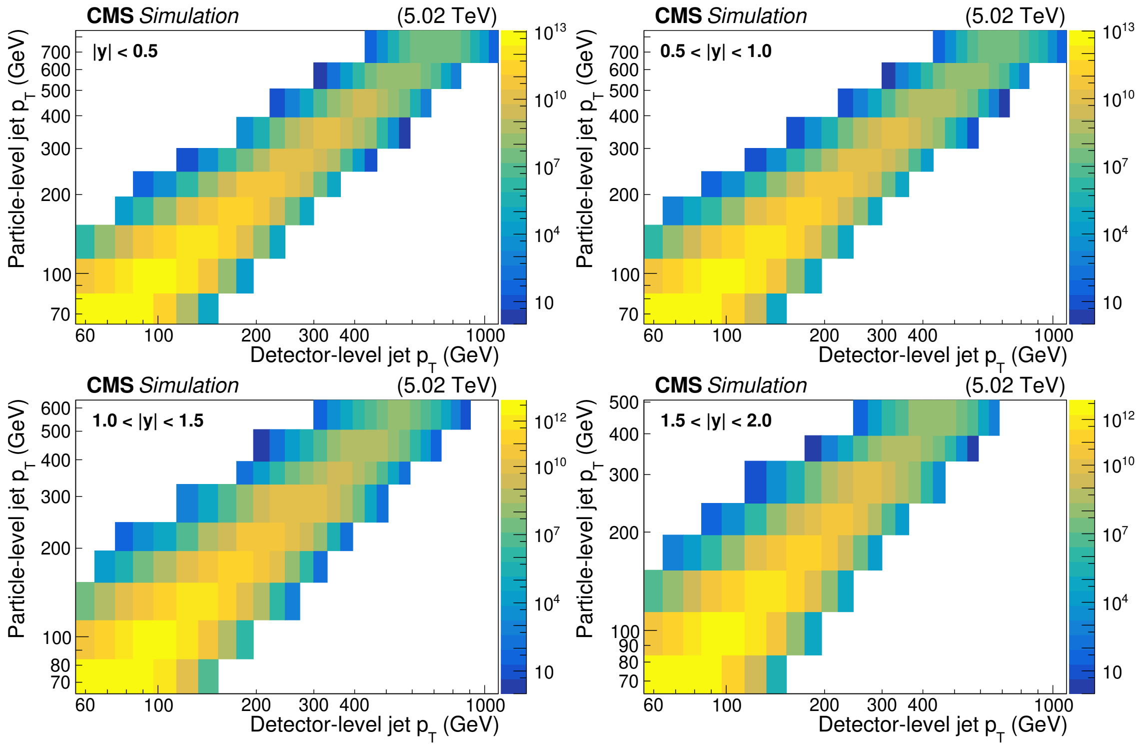

Figure 5. The response matrices for the four rapidity bins. Each 2D-histogram bin contains the number of pseudo-experiment jets that are generated in the particular particle-level p_{T} bin and that are reconstructed in the corresponding detector-level p_{T} bin.

We subtract the fraction of the background, as estimated above, from the detector spectra of figure 2 in order to construct the final detector spectra. We then unfold using the response matrices of figure 5 and covariance matrices of figure 4. Finally, we add the fraction of missed jets to the unfolded spectra to obtain the final particle-level double-differential inclusive jet cross sections to be compared with theoretical predictions. This procedure is repeated for all $|y|$ bins.

Closure tests were performed, where detector-level jet p_T spectra, sampled from the $p_{\mathrm{T}}^{\mathrm{det}}$ pseudo-experiment distributions, are unfolded and they are compared to the corresponding $p_{\mathrm{T}}^{\mathrm{part}}$ distributions. The average agreement over p_T and y bins is $\approx 99.8\%$.

Smoothness tests using the tool of ref. [75] were performed on the unfolded results. Smooth representation of the unfolded cross section p_{T} distributions with $\chi^2/\mathrm{dof} < 1$ is achieved with 3rd and 4th degree Chebyshev polynomials.

10 Systematic uncertainties

10.1 Experimental systematic uncertainties

The main sources of experimental systematic uncertainty are the uncertainty in (i) the JES; (ii) the JER; and (iii) the measured luminosity. Minor sources are the uncertainties in jet identification and the trigger efficiency. All sources are considered uncorrelated and the total experimental systematic uncertainty is derived by summing in quadrature the individual uncertainties.

To estimate the uncertainty in the cross section caused by the uncertainty in the JES, we shift the p_T of all detector-level jets up and down by one standard deviation of the JES uncertainty, determined from a number of different sources of jet energy uncertainty, as described in ref. [45]. The JES uncertainty in jet p_T is about 1.5% for p_T of 50 GeV and reduces to about 0.6% for p_T above 300 GeV. For each p_T shift, we repeat the cross section analysis. This includes the merging of the data sets and using the shifted p_T values to determine if the jet passed the threshold at which the trigger is fully efficient. The new detector-level spectra are unfolded with the default response matrices, and the variations of the resulting measured cross sections per p_T and $|y|$ bin are recorded as the systematic uncertainties.

The JER uncertainty, determined as described in section 4, affects the response matrices used in the unfolding. To estimate the effect, alternative response matrices are obtained for each rapidity bin, by shifting the JER up and down according to the uncertainty in the JER scale factor (10%). We then repeat the unfolding for these two response matrices and record the systematic effect on the unfolded cross sections in all p_T and $|y|$ bins. The use of JER produced from double-sided Crystal Ball functions with the addition of extra tails leads to unfolded results shifted downwards on average by -2.2%, consistently across jet p_T and $|y|$ bins. We increase in quadrature the lower JER systematic uncertainty by this amount. Both the JER and JES systematic uncertainties, as functions of p_T, are smoothed by fitting with smooth functions, in order to maximize the value of this data in future PDF and α_S fits.

The integrated luminosity uncertainty of 2.3% [76, 77] shifts the measured cross sections identically in all p_T and $|y|$ bins. Similarly, the jet identification uncertainty introduces a flat 1% effect [25] on the measured cross section in p_T and $|y|$ bins. Finally, the variation of the thresholds for which each trigger is considered to be fully efficient, leads to a 0.3–0.5% effect on the corresponding threshold p_T bins.

There is a negligible effect on the experimental measurement resulting from the uncertainty in the NP correction, because its effect on the response matrices is extremely small. This is because this analysis is not sensitive to very small variations of the prior distribution in the unfolding process.

Figure 6 shows the effect of JES and JER uncertainties in the unfolded cross sections as functions of p_T and $|y|$, as well as the total systematic effect that includes all uncertainties summed in quadrature. The uncertainty in JES is the largest source of experimental systematic uncertainty. The total effect of the systematic uncertainties in the cross section measurements varies from 4% to 9% depending on the p_T and rapidity bin. The systematic uncertainties of figure 6 originally demonstrated a statistical variation from bin to bin, which was smoothed out by fitting the p_T-dependence.

10.2 Theoretical systematic uncertainties

The main sources of theoretical systematic uncertainties are: (i) the choice of μ_R and μ_F as well as their relationship; (ii) the PDF uncertainty; and (iii) the uncertainty in the NP corrections to the fixed-order calculation. A minor source is the statistical uncertainty from the MC integration.

JHEP01(2025)011

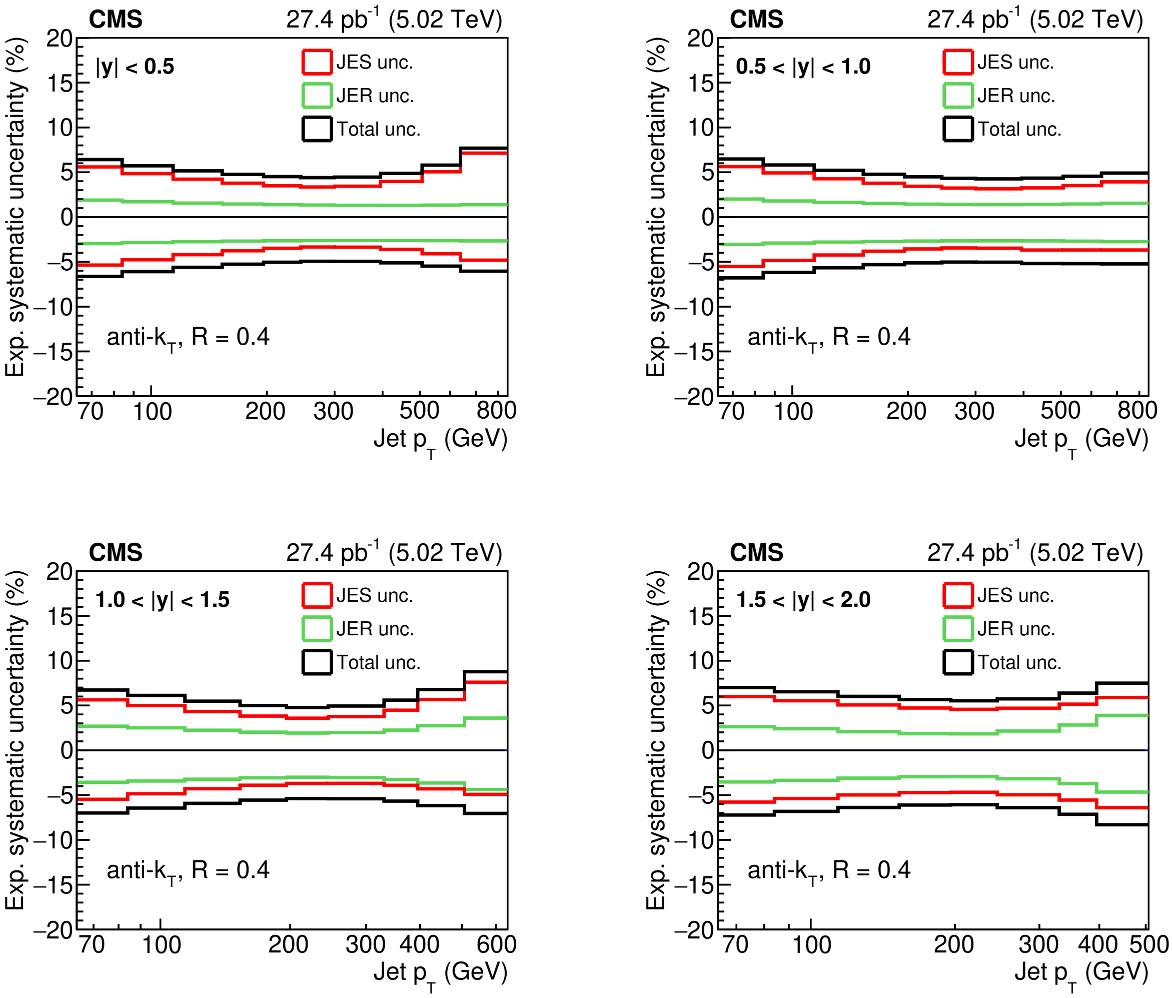

Figure 6. The JES, JER, and total systematic uncertainties in unfolded cross sections as functions of transverse momentum and rapidity. The total systematic uncertainty includes also the luminosity, jet identification and trigger efficiency uncertainties.

In this analysis, for the central cross section prediction, we take $\mu_F = \mu_R = \mu$ and investigate separately the cases where μ is equal to either the p_T of each generated jet or H_T. For each case, the maximum and the minimum variations of the cross section are recorded for the combinations $(\mu_R, \mu_F) = \{(\mu, \mu/2), (\mu/2, \mu), (\mu/2, \mu/2), (\mu, 2\mu), (2\mu, \mu), (2\mu, 2\mu)\}$. The effect depends on the choice of the default scales and is generally larger at higher jet p_T. The same is true for the PDF systematic uncertainty, which is related to the PDF fit that leads to a particular PDF extraction [61, 72]. On the other hand, the NP correction uncertainty affects mostly the jets with lower p_T, as shown in figure 3 for $|y| < 0.5$.

The above sources are considered uncorrelated, and the total theoretical systematic uncertainty is determined by summing in quadrature the individual uncertainties.

The distributions of the theoretical systematic uncertainty in p_T and $|y|$ depend on the fixed-order calculation in pQCD, and the choice of PDF, μ_R, and μ_F; they will be presented in the next section.

JHEP01(2025)011

11 Results and comparisons with theoretical predictions

11.1 Results

Figure 7 shows the unfolded double-differential inclusive particle-level jet cross sections, across 7 orders of magnitude, as functions of p_{T} for the four rapidity bins. The measurements are compared with the theoretical predictions from the NNLO pQCD calculation, with $\mu = H_{\mathrm{T}}$, using the NNPDF3.1NNLO PDF set, and corrected for NP effects. To get these theoretical predictions, we multiply the p_{T}-smooth spline interpolation of the pQCD prediction with the smooth NP corrections, shown in figure 3 for $|y| < 0.5$, and for each bin we integrate this distribution and divide by the bin width. The vertical error bars correspond to the statistical uncertainty in the measurement and the yellow band around the experimental measurement represents the total systematic uncertainty. This systematic uncertainty varies from 4 to 9%, as shown in figure 6, whereas the statistical uncertainty ranges from 0.2% to 27% and becomes dominant above jet p_{T} of 500 GeV for the first three rapidity bins and above 400 GeV for the last one. The red band around the theory prediction shows the total theoretical systematic uncertainty.

11.2 Comparisons with theoretical predictions

The differences between experimental measurements and theoretical predictions are revealed in the ratios of the respective cross sections in all p_{T} bins and $|y|$ bins. Because the sources of experimental and theoretical uncertainties are independent, the respective systematic uncertainties are decoupled. For the purpose of better visual comparisons, we center the experimental uncertainties around the ratio points and the theoretical uncertainties around the line at one. The experimental cross sections and their uncertainties, as well as the uncertainties in the theory, are all divided by a constant theoretical cross section. For these ratios, the uncertainties appear only in the numerators.

Figure 8 shows the ratios of the unfolded inclusive jet cross sections to the NLO theoretical predictions, using the CT18NLO PDF set, with $\mu_{\mathrm{R}} = \mu_{\mathrm{F}} = p_{\mathrm{T}}$, as functions of p_{T}, in the four $|y|$ bins. The theoretical predictions are systematically larger compared to the data, mostly for $|y| < 1.5$.

Figure 9 shows the ratios of the unfolded inclusive jet cross sections to the NLO theoretical predictions, using the CT18NLO PDF set, with $\mu_{\mathrm{R}} = \mu_{\mathrm{F}} = H_{\mathrm{T}}$, as functions of p_{T}, in the four $|y|$ bins. We observe a good agreement between theory and experiment, with data being slightly above the theoretical prediction for $|y| > 1.5$. We also observe larger theoretical systematic uncertainty in the predictions with $\mu = H_{\mathrm{T}}$ compared to $\mu = p_{\mathrm{T}}$, coming from the larger choice of scale magnifying the uncertainties, especially at higher p_{T}.

Figure 10 shows the ratios of the unfolded inclusive jet cross sections to the NNLO theoretical predictions, using the CT18NNLO PDF set, with $\mu_{\mathrm{R}} = \mu_{\mathrm{F}} = H_{\mathrm{T}}$, as functions of p_{T}, in the four $|y|$ bins. We observe a ratio which is less uniform across p_{T}, demonstrating an underestimation from theory at lower p_{T} and an overestimation at higher p_{T}. Also, the theoretical systematic uncertainties at higher p_{T} are smaller for the NNLO prediction, because of the reduced effects of scale variations. The fluctuations in the ratio comes from the statistical uncertainty in the MC integration in the NNLO calculation.

JHEP01(2025)011

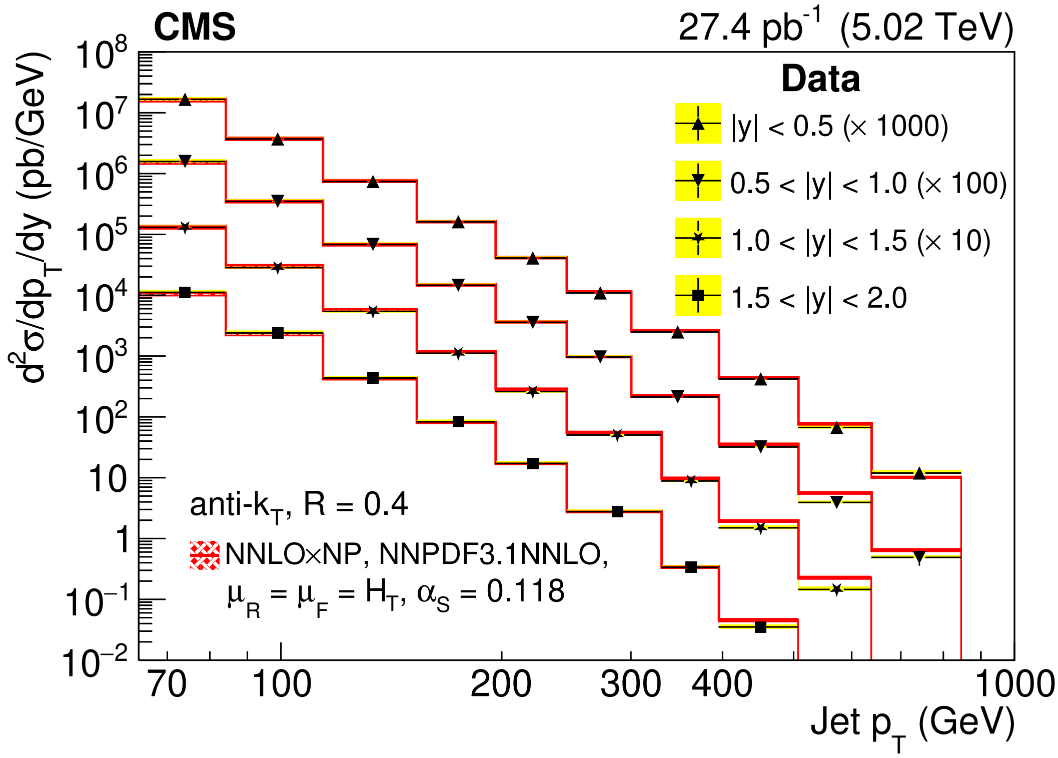

Figure 7. The unfolded measured particle-level inclusive jet cross sections as functions of jet p_{T} in the four rapidity bins (markers), compared to the NNLO perturbative QCD prediction (red histogram), using the NNPDF3.1NNLO PDF set, with $\mu_{\mathrm{R}} = \mu_{\mathrm{F}} = H_{\mathrm{T}}$, and corrected for the NP effects. The yellow (red) band shows the experimental (theoretical) systematic uncertainty. Statistical uncertainties are included but are barely visible.

Figure 11 shows the ratios of the unfolded inclusive jet cross sections to the NNLO theoretical predictions, using the NNPDF3.1NNLO ($\alpha_{\mathrm{S}}(m_{\mathrm{Z}}) = 0.118$) PDF set, for $\mu_{\mathrm{R}} = \mu_{\mathrm{F}} = H_{\mathrm{T}}$, as functions of p_{T}, in the four $|y|$ bins. Compared with the CT18NNLO PDF set, we observe a flatter ratio and a smaller theoretical systematic uncertainty associated with the NNPDF3.1NNLO set. This particular theoretical prediction agrees well with the experimental results for jet $p_{\mathrm{T}} < 400\,\mathrm{GeV}$, both in uniformity of the ratios across p_{T} and their proximity to unity.

Figure 12 shows the effect of $\alpha_{\mathrm{S}}(m_{\mathrm{Z}})$ variation on the NNLO theoretical predictions and the comparison with experimental results, for NNPDF3.1NNLO and $\mu = H_{\mathrm{T}}$. The values of α_{S} range from 0.108 to 0.124. In this plot, the unfolded experimental measurement and all theoretical predictions for different α_{S} choices are divided by a benchmark NNLO theoretical prediction for $\alpha_{\mathrm{S}} = 0.118$ and the same choice of PDFs and scales.

From these results we conclude that the NLO calculation using the CT18NLO PDF set with $\mu = H_{\mathrm{T}}$ agrees better with the experimental measurement than the same calculation with $\mu = p_{\mathrm{T}}$. The latter calculation gives a higher cross section across all p_{T} bins for all $|y|$ bins, maintaining the same shape. On the other hand, the NNLO prediction changes the shape of the ratio for the CT18NNLO PDF set, underestimating the cross section at lower p_{T} bins and overestimating it at higher p_{T} bins, across all $|y|$ bins. The scale systematic uncertainties

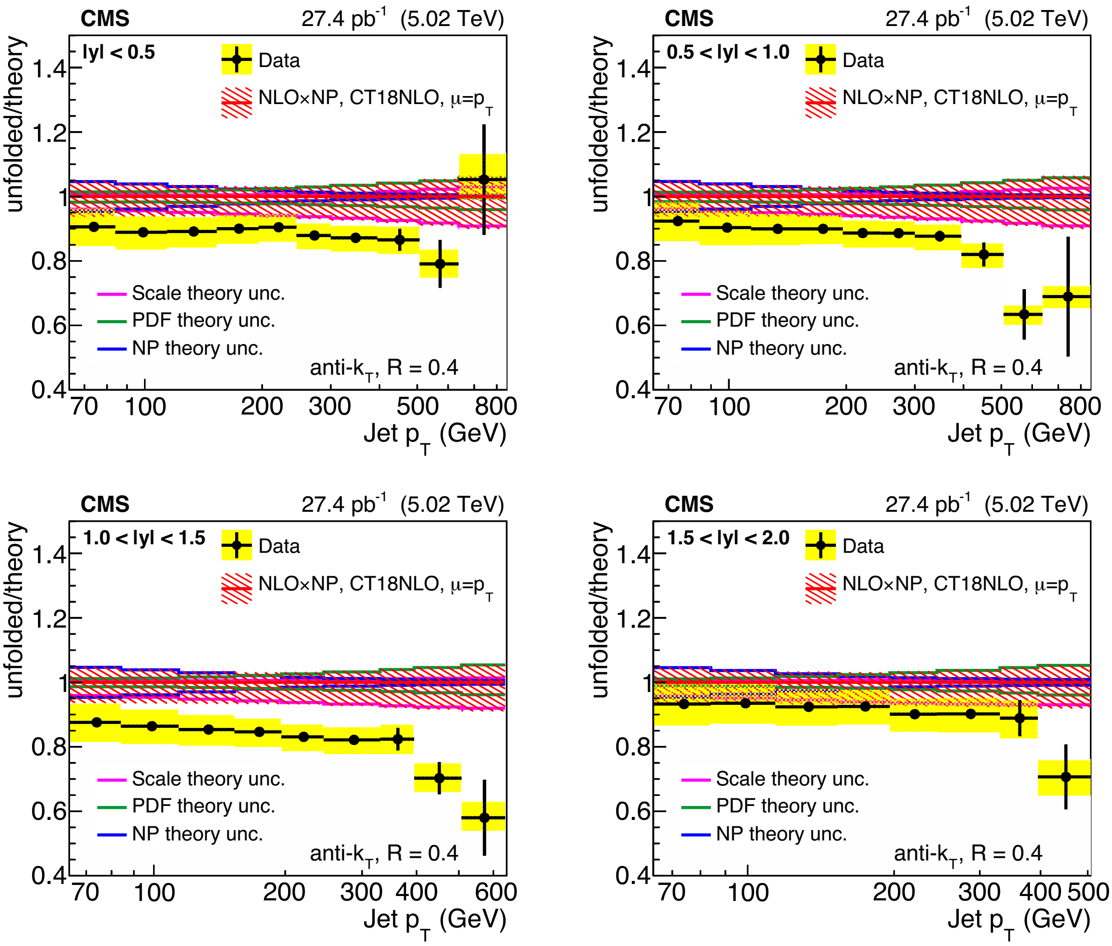

Figure 8. Ratios (points) of the unfolded measured cross sections to the NLO theoretical predictions, using the CT18NLO PDF set, with $\mu = p_{\mathrm{T}}$. The vertical error bars show the statistical experimental uncertainty, the yellow band shows the systematic experimental uncertainty, the hashed red band shows the total theoretical uncertainty, and the individual sources of theoretical uncertainty are shown with colored lines.

are significantly decreased at high p_{T} in NNLO calculations and the NNPDF3.1NNLO PDF set additionally provides small PDF-related systematic uncertainties. These observations provide valuable input to the understanding of jet production, demonstrating how well the data are described by QCD calculations, using various PDF sets, and choices of μ_{R} and μ_{F}.

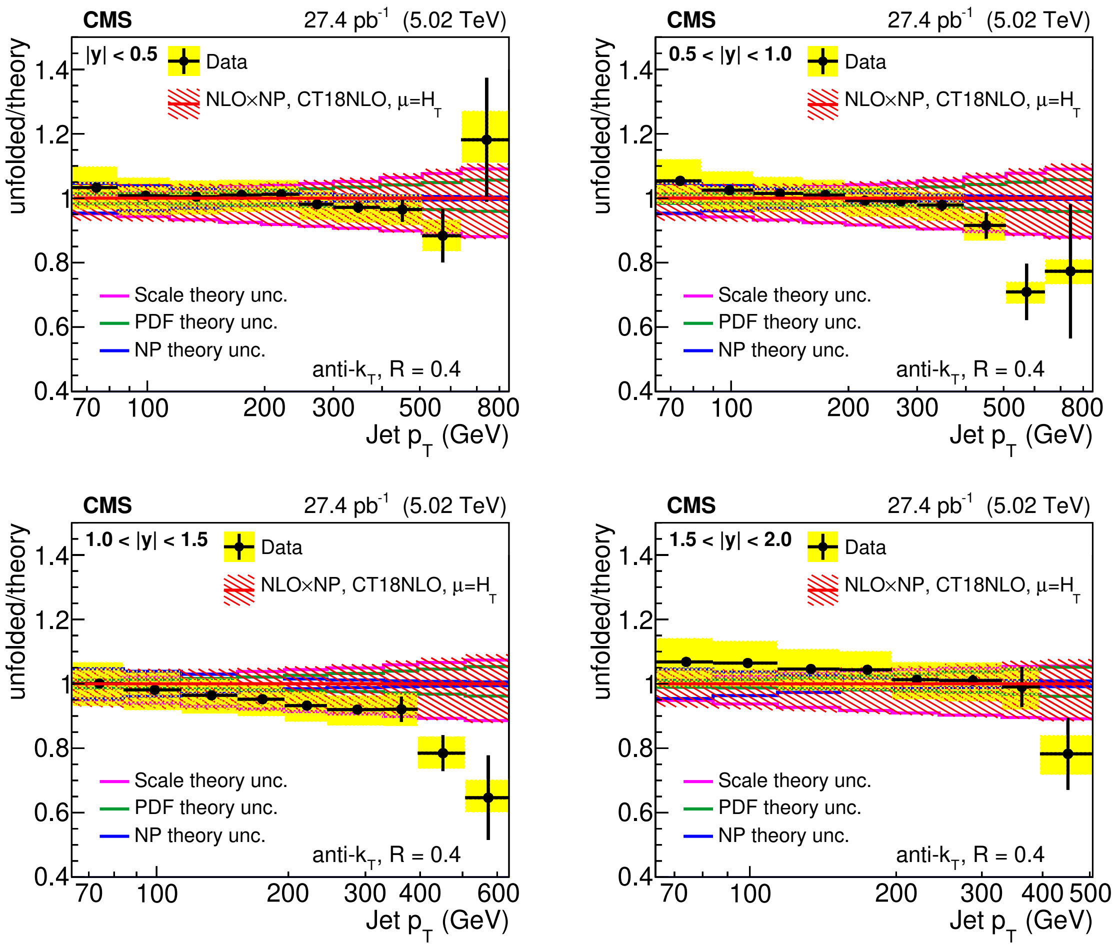

Figure 9. Ratios (points) of the unfolded measured cross sections to the NLO theoretical predictions, using the CT18NLO PDF set, with $\mu = H_{\mathrm{T}}$. The vertical error bars show the statistical experimental uncertainty, the yellow band shows the systematic experimental uncertainty, the hashed red band shows the total theoretical uncertainty, and the individual sources of theoretical uncertainty are shown with colored lines.

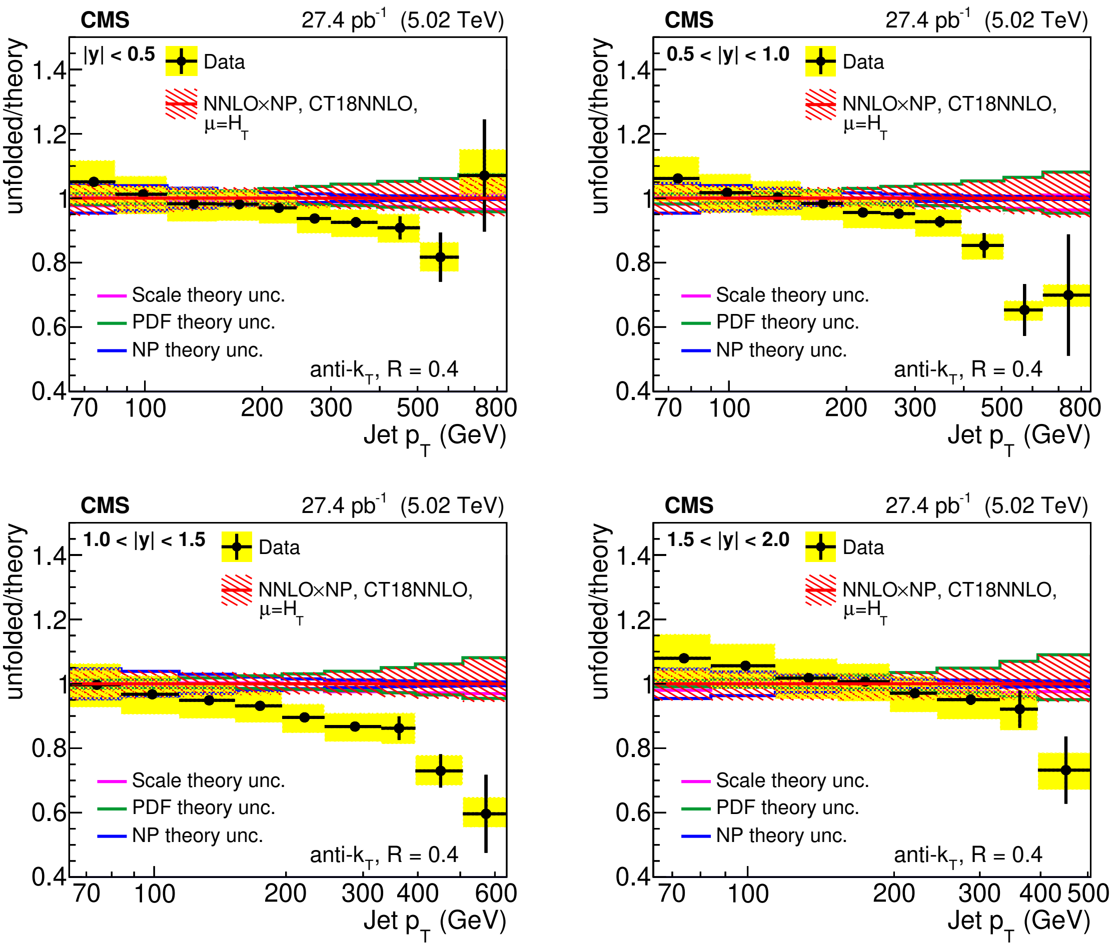

Figure 10. Ratios (points) of the unfolded measured cross sections to the NNLO theoretical predictions, using the CT18NNLO PDF set, with $\mu = H_{\mathrm{T}}$. The vertical error bars show the statistical experimental uncertainty, the yellow band shows the systematic experimental uncertainty, the hashed red band shows the total theoretical uncertainty, and the individual sources of theoretical uncertainty are shown with colored lines.

JHEP01(2025)011

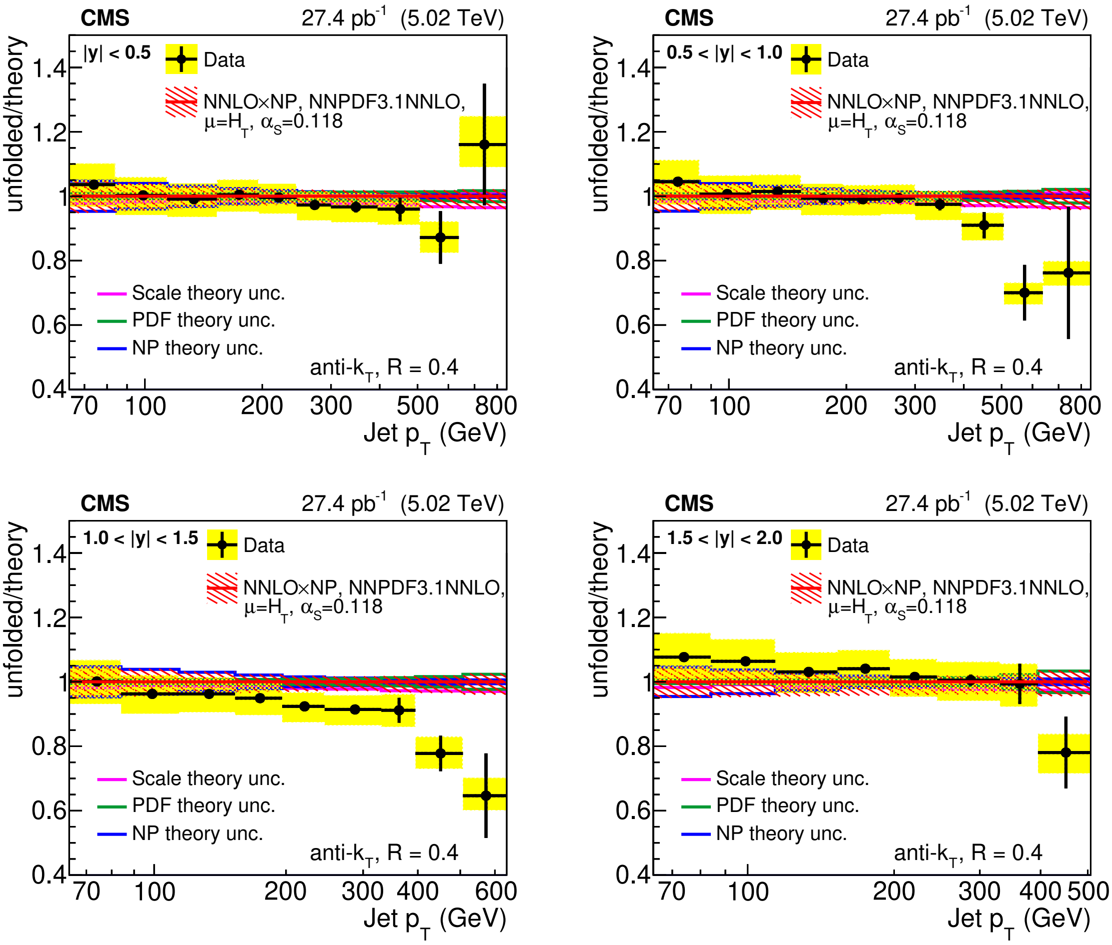

Figure 11. Ratios (points) of the unfolded measured cross sections to the NNLO theoretical predictions, using the NNPDF3.1NNLO PDF set, with $\alpha_S(m_Z) = 0.118$ and $\mu = H_T$. The vertical error bars show the statistical experimental uncertainty, the yellow band shows the systematic experimental uncertainty, the hashed red band shows the total theoretical uncertainty, and the individual sources of theoretical uncertainty are shown with colored lines.

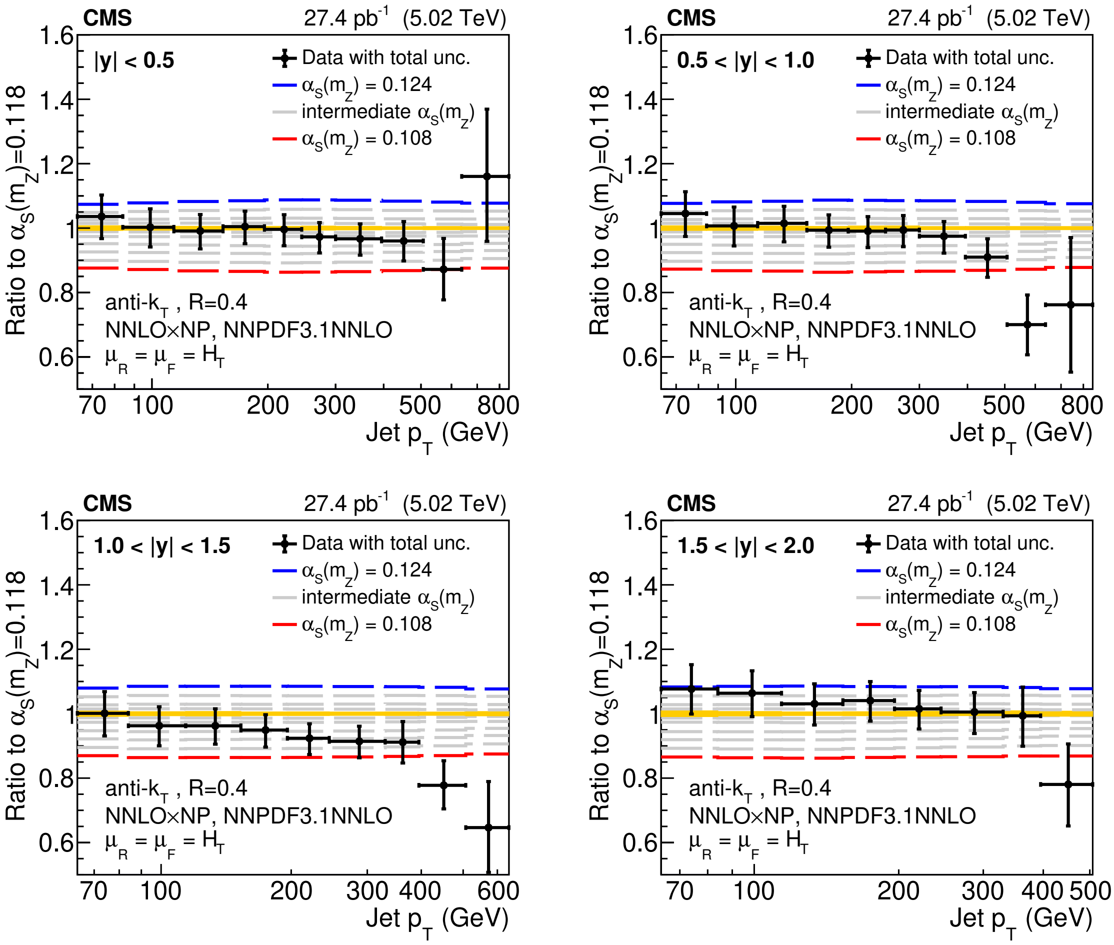

Figure 12. The effect of $\alpha_S(m_Z)$ variation. The NNLO theoretical cross section predictions using the NNPDF3.1NNLO PDF with $\mu = H_T$, calculated for different choices of α_S (0.108, 0.110, 0.112, 0.114, 0.116, 0.117, 0.118, 0.119, 0.120, 0.122, and 0.124), are divided by the benchmark NNLO prediction for $\alpha_S = 0.118$ and the same choice of PDF set, μ_R, and μ_F. Also shown is the experimental unfolded measurement divided by the same benchmark prediction. The width of the unity line corresponds to the statistical uncertainty from the MC integration for the determination of the NNLO prediction. The error bars on the unfolded data correspond to the total experimental statistical and systematic uncertainty added in quadrature.

12 Summary

The double-differential inclusive jet cross section in proton-proton collisions at 5.02 TeV was measured in the rapidity interval $|y| < 2$, and for the transverse momentum range $0.06 < p_T < 1$ TeV. The achieved experimental systematic uncertainty is about 5% across most p_T ranges for all $|y|$. The next-to-leading order (NLO) perturbative quantum chromodynamics calculations agree better with the observations if the renormalization and factorization scales (μ) equal H_T, the scalar sum of the transverse momentum (p_T) of the partons in each event. The energy scale systematic uncertainty also increases when the scale is changed from $\mu = p_T$ of each jet to $\mu = H_T$ in the NLO case. Changing the order of the perturbative calculation from the NLO to next-to-NLO (NNLO) reduces the scale systematic uncertainty at high

JHEP01(2025)011

p_{T}, but increases it at low p_{T}. The effect of changing the scale is not very large for the NNLO calculation, and the scale systematic decreases at low p_{T} when the scale is changed from $\mu = p_{\mathrm{T}}$ to $\mu = H_{\mathrm{T}}$. The uncertainty in the predicted cross section due to the parton distribution functions is significantly reduced by choosing the NNPDF3.1NNLO set. The measurement is consistent with NLO and the more precise NNLO prediction.

Acknowledgments

We thank João Pires for his work on the NNLO pQCD predictions.

We congratulate our colleagues in the CERN accelerator departments for the excellent performance of the LHC and thank the technical and administrative staffs at CERN and at other CMS institutes for their contributions to the success of the CMS effort. In addition, we gratefully acknowledge the computing centers and personnel of the Worldwide LHC Computing Grid and other centers for delivering so effectively the computing infrastructure essential to our analyses. Finally, we acknowledge the enduring support for the construction and operation of the LHC, the CMS detector, and the supporting computing infrastructure provided by the following funding agencies: SC (Armenia), BMBWF and FWF (Austria); FNRS and FWO (Belgium); CNPq, CAPES, FAPERJ, FAPERGS, and FAPESP (Brazil); MES and BNSF (Bulgaria); CERN; CAS, MoST, and NSFC (China); MINCIENCIAS (Colombia); MSES and CSF (Croatia); RIF (Cyprus); SENESCYT (Ecuador); MoER, ERC PUT and ERDF (Estonia); Academy of Finland, MEC, and HIP (Finland); CEA and CNRS/IN2P3 (France); SRNSF (Georgia); BMBF, DFG, and HGF (Germany); GSRI (Greece); NKFIH (Hungary); DAE and DST (India); IPM (Iran); SFI (Ireland); INFN (Italy); MSIP and NRF (Republic of Korea); MES (Latvia); LAS (Lithuania); MOE and UM (Malaysia); BUAP, CINVESTAV, CONACYT, LNS, SEP, and UASLP-FAI (Mexico); MOS (Montenegro); MBIE (New Zealand); PAEC (Pakistan); MES and NSC (Poland); FCT (Portugal); MESTD (Serbia); MCIN/AEI and PCTI (Spain); MOSTR (Sri Lanka); Swiss Funding Agencies (Switzerland); MST (Taipei); MHESI and NSTDA (Thailand); TUBITAK and TENMAK (Turkey); NASU (Ukraine); STFC (United Kingdom); DOE and NSF (U.S.A.).

Individuals have received support from the Marie-Curie program and the European Research Council and Horizon 2020 Grant, contract Nos. 675440, 724704, 752730, 758316, 765710, 824093, and COST Action CA16108 (European Union); the Leventis Foundation; the Alfred P. Sloan Foundation; the Alexander von Humboldt Foundation; the Science Committee, project no. 22rl-037 (Armenia); the Belgian Federal Science Policy Office; the Fonds pour la Formation à la Recherche dans l'Industrie et dans l'Agriculture (FRIA-Belgium); the Agentschap voor Innovatie door Wetenschap en Technologie (IWT-Belgium); the F.R.S.-FNRS and FWO (Belgium) under the "Excellence of Science — EOS" — be.h project n. 30820817; the Beijing Municipal Science & Technology Commission, No. Z191100007219010 and Fundamental Research Funds for the Central Universities (China); the Ministry of Education, Youth and Sports (MEYS) of the Czech Republic; the Shota Rustaveli National Science Foundation, grant FR-22-985 (Georgia); the Deutsche Forschungsgemeinschaft (DFG), under Germany's Excellence Strategy — EXC 2121 "Quantum Universe" — 390833306, and under project number 400140256 — GRK2497; the Hellenic Foundation for Research and Innovation (HFRI), Project Number 2288 (Greece); the Hungarian Academy of Sciences, the New National Excellence Program — ÚNKP, the NKFIH research grants K 124845, K 124850, K 128713, K 128786, K 129058, K 131991, K 133046, K 138136, K 143460, K 143477, 2020-2.2.1-ED-2021-00181, and TKP2021-NKTA-64 (Hungary); the Council of Science and Industrial Research, India; ICSC — National Research Center for High Performance Computing, Big Data and Quantum Computing, funded by the EU NexGeneration program (Italy); the Latvian Council of Science; the Ministry of Education and Science, project no. 2022/WK/14, and the National Science Center, contracts Opus 2021/41/B/ST2/01369 and 2021/43/B/ST2/01552 (Poland); the Fundação para a Ciência e a Tecnologia, grant CEECIND/01334/2018 (Portugal); the National Priorities Research Program by Qatar National Research Fund; MCIN/AEI/10.13039/501100011033, ERDF "a way of making Europe", and the Programa Estatal de Fomento de la Investigación Científica y Técnica de Excelencia María de Maeztu, grant MDM-2017-0765 and Programa Severo Ochoa del Principado de Asturias (Spain); the Chulalongkorn Academic into Its 2nd Century Project Advancement Project, and the National Science, Research and Innovation Fund via the Program Management Unit for Human Resources & Institutional Development, Research and Innovation, grant B37G660013 (Thailand); the Kavli Foundation; the Nvidia Corporation; the SuperMicro Corporation; the Welch Foundation, contract C-1845; and the Weston Havens Foundation (U.S.A.).

Data Availability Statement. Release and preservation of data used by the CMS Collaboration as the basis for publications is guided by the CMS data preservation, re-use, and open access policy.

Code Availability Statement. The CMS core software is publicly available on GitHub.

References

[1] Axial Field Spectrometer collaboration, *The jet cross-section in pp interactions at* $\sqrt{s} = 45$ *GeV and its* $\sqrt{s}$ *dependence*, *Phys. Lett. B* **123** (1983) 133 [inSPIRE].

[2] Axial Field Spectrometer collaboration, *Direct evidence for the emergence of jets in events triggered on large transverse energy in pp collisions at* $\sqrt{s} = 63$ *GeV*, *Phys. Lett. B* **118** (1982) 185 [inSPIRE].

[3] UA1 collaboration, *Hadronic jet production at the CERN proton-anti-proton collider*, *Phys. Lett. B* **132** (1983) 214 [inSPIRE].

[4] UA2 collaboration, *Measurement of the* $\sqrt{s}$ *dependence of jet production at the CERN anti-p p collider*, *Phys. Lett. B* **160** (1985) 349 [inSPIRE].

[5] UA1 collaboration, *Measurement of the inclusive jet cross-section at the CERN p anti-p collider*, *Phys. Lett. B* **172** (1986) 461 [inSPIRE].

[6] UA2 collaboration, *Inclusive jet cross-section and a search for quark compositeness at the CERN* $\bar{p}p$ *collider*, *Phys. Lett. B* **257** (1991) 232 [inSPIRE].

[7] UA1 collaboration, *Production of low transverse energy clusters in anti-p p collisions at* $\sqrt{s} = 0.2$ *TeV to* 0.9 *TeV and their interpretation in terms of QCD jets*, Nucl. Phys. B **309** (1988) 405 [INSPIRE].

[8] CDF collaboration, *Comparison of jet production in* $\bar{p}p$ *collisions at* $\sqrt{s} = 546$ *GeV and* 1800 *GeV*, Phys. Rev. Lett. **70** (1993) 1376 [INSPIRE].

[9] A.A. Bhatti, *Inclusive jet production at* $\sqrt{s} = 630$ *GeV and a test of scaling at CDF*, in *1996 Annual Divisional Meeting (DPF96) of the Division of Particles and Fields of the American Physical Society*, Minnesota, MN, U.S.A. August 10–15 1996.

[10] D0 collaboration, *The ratio of jet cross sections at* $\sqrt{s} = 630$ *GeV and* 1800 *GeV*, Phys. Rev. Lett. **86** (2001) 2523 [hep-ex/0008072] [INSPIRE].

[11] CDF collaboration, *Inclusive jet cross section in* $\bar{p}p$ *collisions at* $\sqrt{s} = 1.8$ *TeV*, Phys. Rev. Lett. **77** (1996) 438 [hep-ex/9601008] [INSPIRE].

[12] D0 collaboration, *Inclusive jet production in* $p\bar{p}$ *collisions*, Phys. Rev. Lett. **86** (2001) 1707 [hep-ex/0011036] [INSPIRE].

[13] CDF collaboration, *Measurement of the inclusive jet cross section using the* $k_{\rm T}$ *algorithm in p anti-p collisions at* $\sqrt{s} = 1.96$ *TeV*, Phys. Rev. Lett. **96** (2006) 122001 [hep-ex/0512062] [INSPIRE].

[14] CDF collaboration, *Measurement of the inclusive jet cross section using the* $k_{\rm T}$ *algorithmin* $p\bar{p}$ *collisions at* $\sqrt{s} = 1.96$ *TeV with the CDF II detector*, Phys. Rev. D **75** (2007) 092006 [*Erratum ibid.* **75** (2007) 119901] [hep-ex/0701051] [INSPIRE].

[15] CDF collaboration, *Measurement of the inclusive jet cross section at the Fermilab Tevatron p anti-p collider using a cone-based jet algorithm*, Phys. Rev. D **78** (2008) 052006 [*Erratum ibid.* **79** (2009) 119902] [arXiv:0807.2204] [INSPIRE].

[16] D0 collaboration, *Measurement of the inclusive jet cross-section in* $p\bar{p}$ *collisions at* $\sqrt{s} = 1.96$ *TeV*, Phys. Rev. Lett. **101** (2008) 062001 [arXiv:0802.2400] [INSPIRE].

[17] D0 collaboration, *Measurement of the inclusive jet cross section in* $p\bar{p}$ *collisions at* $\sqrt{s} = 1.96$ *TeV*, Phys. Rev. D **85** (2012) 052006 [arXiv:1110.3771] [INSPIRE].

[18] ALICE collaboration, *Measurement of the inclusive differential jet cross section in pp collisions at* $\sqrt{s} = 2.76$ *TeV*, Phys. Lett. B **722** (2013) 262 [arXiv:1301.3475] [INSPIRE].

[19] ATLAS collaboration, *Measurement of the inclusive jet cross section in pp collisions at* $\sqrt{s} = 2.76$ *TeV and comparison to the inclusive jet cross section at* $\sqrt{s} = 7$ *TeV using the ATLAS detector*, Eur. Phys. J. C **73** (2013) 2509 [arXiv:1304.4739] [INSPIRE].

[20] CMS collaboration, *Measurement of the inclusive jet cross section in pp collisions at* $\sqrt{s} = 2.76$ *TeV*, Eur. Phys. J. C **76** (2016) 265 [arXiv:1512.06212] [INSPIRE].

[21] ATLAS collaboration, *Measurement of inclusive jet and dijet cross sections in proton-proton collisions at 7 TeV centre-of-mass energy with the ATLAS detector*, Eur. Phys. J. C **71** (2011) 1512 [arXiv:1009.5908] [INSPIRE].

[22] CMS collaboration, *Measurement of the inclusive jet cross section in pp collisions at* $\sqrt{s} = 7$ *TeV*, Phys. Rev. Lett. **107** (2011) 132001 [arXiv:1106.0208] [INSPIRE].

[23] ATLAS collaboration, *Measurement of inclusive jet and dijet production in pp collisions at* $\sqrt{s} = 7$ *TeV using the ATLAS detector*, Phys. Rev. D **86** (2012) 014022 [arXiv:1112.6297] [INSPIRE].

JHEP01(2025)011

[24] CMS collaboration, *Measurements of differential jet cross sections in proton-proton collisions at $\sqrt{s} = 7$ TeV with the CMS detector*, Phys. Rev. D **87** (2013) 112002 [*Erratum ibid.* **87** (2013) 119902] [arXiv:1212.6660] [INSPIRE].

[25] CMS collaboration, *Measurement of the ratio of inclusive jet cross sections using the anti-k_T algorithm with radius parameters $R = 0.5$ and 0.7 in pp collisions at $\sqrt{s} = 7$ TeV*, Phys. Rev. D **90** (2014) 072006 [arXiv:1406.0324] [INSPIRE].

[26] ATLAS collaboration, *Measurement of the inclusive jet cross-section in proton-proton collisions at $\sqrt{s} = 7$ TeV using $4.5\,fb^{-1}$ of data with the ATLAS detector*, JHEP **02** (2015) 153 [*Erratum ibid.* **09** (2015) 141] [arXiv:1410.8857] [INSPIRE].

[27] CMS collaboration, *Constraints on parton distribution functions and extraction of the strong coupling constant from the inclusive jet cross section in pp collisions at $\sqrt{s} = 7$ TeV*, Eur. Phys. J. C **75** (2015) 288 [arXiv:1410.6765] [INSPIRE].

[28] CMS collaboration, *Measurement and QCD analysis of double-differential inclusive jet cross sections in pp collisions at $\sqrt{s} = 8$ TeV and cross section ratios to 2.76 and 7 TeV*, JHEP **03** (2017) 156 [arXiv:1609.05331] [INSPIRE].

[29] ATLAS collaboration, *Measurement of the inclusive jet cross-sections in proton-proton collisions at $\sqrt{s} = 8$ TeV with the ATLAS detector*, JHEP **09** (2017) 020 [arXiv:1706.03192] [INSPIRE].

[30] CMS collaboration, *Measurement of the double-differential inclusive jet cross section in proton-proton collisions at $\sqrt{s} = 13$ TeV*, Eur. Phys. J. C **76** (2016) 451 [arXiv:1605.04436] [INSPIRE].

[31] ATLAS collaboration, *Measurement of inclusive jet and dijet cross-sections in proton-proton collisions at $\sqrt{s} = 13$ TeV with the ATLAS detector*, JHEP **05** (2018) 195 [arXiv:1711.02692] [INSPIRE].

[32] CMS collaboration, *Dependence of inclusive jet production on the anti-k_T distance parameter in pp collisions at $\sqrt{s} = 13$ TeV*, JHEP **12** (2020) 082 [arXiv:2005.05159] [INSPIRE].

[33] CMS collaboration, *Measurement and QCD analysis of double-differential inclusive jet cross sections in proton-proton collisions at $\sqrt{s} = 13$ TeV*, JHEP **02** (2022) 142 [*Addendum ibid.* **12** (2022) 035] [arXiv:2111.10431] [INSPIRE].

[34] WA97 collaboration, *Strangeness enhancement at mid-rapidity in Pb Pb collisions at 158 A-GeV/c*, Phys. Lett. B **449** (1999) 401 [INSPIRE].

[35] WA97 collaboration, *Transverse mass spectra of strange and multistrange particles in Pb Pb collisions at 158 A-GeV/c*, Eur. Phys. J. C **14** (2000) 633 [INSPIRE].

[36] CMS collaboration, *Evidence for collectivity in pp collisions at the LHC*, Phys. Lett. B **765** (2017) 193 [arXiv:1606.06198] [INSPIRE].

[37] CMS collaboration, *First measurement of large area jet transverse momentum spectra in heavy-ion collisions*, JHEP **05** (2021) 284 [arXiv:2102.13080] [INSPIRE].

[38] CMS collaboration, *Measurement of inclusive jet production and nuclear modifications in pPb collisions at $\sqrt{s_{NN}} = 5.02$ TeV*, Eur. Phys. J. C **76** (2016) 372 [arXiv:1601.02001] [INSPIRE].

[39] D. d'Enterria, *Jet quenching*, Landolt-Bornstein **23** (2010) 471 [arXiv:0902.2011] [INSPIRE].

[40] CMS collaboration, *Measurement of the splitting function in pp and Pb-Pb collisions at $\sqrt{s_{NN}} = 5.02$ TeV*, Phys. Rev. Lett. **120** (2018) 142302 [arXiv:1708.09429] [INSPIRE].

[41] CMS collaboration, *Observation of medium-induced modifications of jet fragmentation in Pb-Pb collisions at $\sqrt{s_{NN}} = 5.02$ TeV using isolated photon-tagged jets*, Phys. Rev. Lett. **121** (2018) 242301 [arXiv:1801.04895] [INSPIRE].

[42] ATLAS collaboration, *Observation of a centrality-dependent dijet asymmetry in lead-lead collisions at $\sqrt{s_{NN}} = 2.77$ TeV with the ATLAS detector at the LHC*, Phys. Rev. Lett. **105** (2010) 252303 [arXiv:1011.6182] [INSPIRE].

[43] CMS collaboration, *Jet momentum dependence of jet quenching in PbPb collisions at $\sqrt{s_{NN}} = 2.76$ TeV*, Phys. Lett. B **712** (2012) 176 [arXiv:1202.5022] [INSPIRE].

[44] *HEPData record for this analysis*, , (2024).

[45] CMS collaboration, *Jet energy scale and resolution in the CMS experiment in pp collisions at 8 TeV*, 2017 *JINST* **12** P02014 [arXiv:1607.03663] [INSPIRE].

[46] CMS collaboration, *The CMS trigger system*, 2017 *JINST* **12** P01020 [arXiv:1609.02366] [INSPIRE].

[47] CMS collaboration, *Performance of the CMS Level-1 trigger in proton-proton collisions at $\sqrt{s} = 13$ TeV*, 2020 *JINST* **15** P10017 [arXiv:2006.10165] [INSPIRE].

[48] V. Gori, *The CMS high level trigger*, Int. J. Mod. Phys. Conf. Ser. **31** (2014) 1460297 [arXiv:1403.1500] [INSPIRE].

[49] CMS collaboration, *The CMS experiment at the CERN LHC*, 2008 *JINST* **3** S08004 [INSPIRE].

[50] CMS collaboration, *Particle-flow reconstruction and global event description with the CMS detector*, 2017 *JINST* **12** P10003 [arXiv:1706.04965] [INSPIRE].

[51] M. Cacciari, G.P. Salam and G. Soyez, *The anti-k_t jet clustering algorithm*, JHEP **04** (2008) 063 [arXiv:0802.1189] [INSPIRE].

[52] M. Cacciari, G.P. Salam and G. Soyez, *FastJet user manual*, Eur. Phys. J. C **72** (2012) 1896 [arXiv:1111.6097] [INSPIRE].

[53] D. Contardo et al., *Technical proposal for the phase-II upgrade of the CMS detector*, CERN-LHCC-2015-010, CERN, Geneva, Switzerland (2015) [DOI:10.17181/CERN.VU8I.D59J].

[54] CMS collaboration, *Determination of jet energy calibration and transverse momentum resolution in CMS*, 2011 *JINST* **6** P11002 [arXiv:1107.4277] [INSPIRE].

[55] T. Sjöstrand et al., *An introduction to PYTHIA 8.2*, Comput. Phys. Commun. **191** (2015) 159 [arXiv:1410.3012] [INSPIRE].

[56] B. Andersson, *The Lund model*, Cambridge University Press, Cambridge, U.K. (1998) [DOI:10.1017/9781009401296] [INSPIRE].

[57] NNPDF collaboration, *A determination of parton distributions with faithful uncertainty estimation*, Nucl. Phys. B **809** (2009) 1 [*Erratum ibid.* **816** (2009) 293] [arXiv:0808.1231] [INSPIRE].

[58] P. Skands, S. Carrazza and J. Rojo, *Tuning PYTHIA 8.1: the Monash 2013 tune*, Eur. Phys. J. C **74** (2014) 3024 [arXiv:1404.5630] [INSPIRE].

[59] CMS collaboration, *Event generator tunes obtained from underlying event and multiparton scattering measurements*, Eur. Phys. J. C **76** (2016) 155 [arXiv:1512.00815] [INSPIRE].

[60] J. Bellm et al., *Herwig 7.0/Herwig++ 3.0 release note*, Eur. Phys. J. C **76** (2016) 196 [arXiv:1512.01178] [INSPIRE].

[61] NNPDF collaboration, *Parton distributions from high-precision collider data*, Eur. Phys. J. C **77** (2017) 663 [arXiv:1706.00428] [INSPIRE].

[62] B.R. Webber, *A QCD model for jet fragmentation including soft gluon interference*, Nucl. Phys. B **238** (1984) 492 [INSPIRE].

[63] CMS collaboration, *Development and validation of HERWIG 7 tunes from CMS underlying-event measurements*, Eur. Phys. J. C **81** (2021) 312 [arXiv:2011.03422] [INSPIRE].

[64] GEANT4 collaboration, *GEANT4 — a simulation toolkit*, Nucl. Instrum. Meth. A **506** (2003) 250 [INSPIRE].

[65] Z. Nagy, *Three jet cross-sections in hadron hadron collisions at next-to-leading order*, Phys. Rev. Lett. **88** (2002) 122003 [hep-ph/0110315] [INSPIRE].

[66] Z. Nagy, *Next-to-leading order calculation of three jet observables in hadron hadron collision*, Phys. Rev. D **68** (2003) 094002 [hep-ph/0307268] [INSPIRE].

[67] T. Gehrmann et al., *Jet cross sections and transverse momentum distributions with NNLOJET*, PoS **RADCOR2017** (2018) 074 [arXiv:1801.06415] [INSPIRE].

[68] J. Currie, E.W.N. Glover and J. Pires, *Next-to-next-to leading order QCD predictions for single jet inclusive production at the LHC*, Phys. Rev. Lett. **118** (2017) 072002 [arXiv:1611.01460] [INSPIRE].

[69] J. Currie et al., *Infrared sensitivity of single jet inclusive production at hadron colliders*, JHEP **10** (2018) 155 [arXiv:1807.03692] [INSPIRE].

[70] D. Britzger et al., *Calculations for deep inelastic scattering using fast interpolation grid techniques at NNLO in QCD and the extraction of α_s from HERA data*, Eur. Phys. J. C **79** (2019) 845 [*Erratum ibid.* **81** (2021) 957] [arXiv:1906.05303] [INSPIRE].

[71] FASTNLO collaboration, *New features in version 2 of the fastNLO project*, in the proceedings of the *20th International Workshop on Deep-Inelastic Scattering and Related Subjects*, (2012) [DOI:10.3204/DESY-PROC-2012-02/165] [arXiv:1208.3641] [INSPIRE].

[72] T.-J. Hou et al., *New CTEQ global analysis of quantum chromodynamics with high-precision data from the LHC*, Phys. Rev. D **103** (2021) 014013 [arXiv:1912.10053] [INSPIRE].

[73] A. Buckley et al., *LHAPDF6: parton density access in the LHC precision era*, Eur. Phys. J. C **75** (2015) 132 [arXiv:1412.7420] [INSPIRE].

[74] S. Schmitt, *TUnfold: an algorithm for correcting migration effects in high energy physics*, 2012 JINST **7** T10003 [arXiv:1205.6201] [INSPIRE].

[75] P.L.S. Connor and R. Žlebčík, *STEP: a tool to perform tests of smoothness on differential distributions based on expansion of polynomials*, SciPost Phys. Core **6** (2023) 040 [arXiv:2111.09968] [INSPIRE].

[76] CMS collaboration, *CMS luminosity calibration for the pp reference run at $\sqrt{s} = 5.02$ TeV*, CMS-PAS-LUM-16-001, CERN, Geneva, Switzerland (2016).

[77] CMS collaboration, *Precision luminosity measurement in proton-proton collisions at $\sqrt{s} = 13$ TeV in 2015 and 2016 at CMS*, Eur. Phys. J. C **81** (2021) 800 [arXiv:2104.01927] [INSPIRE].

JHEP01(2025)011

The CMS collaboration

Yerevan Physics Institute, Yerevan, Armenia
A. Hayrapetyan, A. Tumasyan[1]

Institut für Hochenergiephysik, Vienna, Austria
W. Adam, J.W. Andrejkovic, T. Bergauer, S. Chatterjee, K. Damanakis, M. Dragicevic, A. Escalante Del Valle, P.S. Hussain, M. Jeitler[2], N. Krammer, L. Lechner, D. Liko, I. Mikulec, J. Schieck[2], R. Schöfbeck, D. Schwarz, M. Sonawane, S. Templ, W. Waltenberger, C.-E. Wulz[2]

Universiteit Antwerpen, Antwerpen, Belgium
M.R. Darwish[3], T. Janssen, T. Kello[4], P. Van Mechelen

Vrije Universiteit Brussel, Brussel, Belgium
E.S. Bols, J. D'Hondt, A. De Moor, M. Delcourt, H. El Faham, S. Lowette, I. Makarenko, A. Morton, D. Müller, A.R. Sahasransu, S. Tavernier, S. Van Putte, D. Vannerom

Université Libre de Bruxelles, Bruxelles, Belgium
B. Clerbaux, S. Dansana, G. De Lentdecker, L. Favart, D. Hohov, J. Jaramillo, K. Lee, M. Mahdavikhorrami, A. Malara, S. Paredes, L. Pétré, N. Postiau, L. Thomas, M. Vanden Bemden, C. Vander Velde, P. Vanlaer

Ghent University, Ghent, Belgium
M. De Coen, D. Dobur, J. Knolle, L. Lambrecht, G. Mestdach, C. Rendón, A. Samalan, K. Skovpen, M. Tytgat, N. Van Den Bossche, B. Vermassen, L. Wezenbeek

Université Catholique de Louvain, Louvain-la-Neuve, Belgium
A. Benecke, G. Bruno, F. Bury, C. Caputo, C. Delaere, I.S. Donertas, A. Giammanco, K. Jaffel, Sa. Jain, V. Lemaitre, J. Lidrych, P. Mastrapasqua, K. Mondal, T.T. Tran, P. Vischia, S. Wertz

Centro Brasileiro de Pesquisas Fisicas, Rio de Janeiro, Brazil
G.A. Alves, E. Coelho, C. Hensel, A. Moraes, P. Rebello Teles

Universidade do Estado do Rio de Janeiro, Rio de Janeiro, Brazil
W.L. Aldá Júnior, M. Alves Gallo Pereira, M. Barroso Ferreira Filho, H. Brandao Malbouisson, W. Carvalho, J. Chinellato[5], E.M. Da Costa, G.G. Da Silveira[6], D. De Jesus Damiao, V. Dos Santos Sousa, S. Fonseca De Souza, J. Martins[7], C. Mora Herrera, K. Mota Amarilo, L. Mundim, H. Nogima, A. Santoro, S.M. Silva Do Amaral, A. Sznajder, M. Thiel, A. Vilela Pereira

Universidade Estadual Paulista, Universidade Federal do ABC, São Paulo, Brazil
C.A. Bernardes[6], L. Calligaris, T.R. Fernandez Perez Tomei, E.M. Gregores, P.G. Mercadante, S.F. Novaes, B. Orzari, Sandra S. Padula

Institute for Nuclear Research and Nuclear Energy, Bulgarian Academy of Sciences, Sofia, Bulgaria
A. Aleksandrov, G. Antchev, R. Hadjiiska, P. Iaydjiev, M. Misheva, M. Shopova, G. Sultanov

University of Sofia, Sofia, Bulgaria
A. Dimitrov, T. Ivanov, L. Litov, B. Pavlov, P. Petkov, A. Petrov, E. Shumka

Instituto De Alta Investigación, Universidad de Tarapacá, Casilla 7 D, Arica, Chile
S. Keshri, S. Thakur

Beihang University, Beijing, China
T. Cheng, Q. Guo, T. Javaid[8], M. Mittal, L. Yuan

Department of Physics, Tsinghua University, Beijing, China
G. Bauer[9], Z. Hu, S. Lezki, K. Yi[9,10]

Institute of High Energy Physics, Beijing, China
G.M. Chen[8], H.S. Chen[8], M. Chen[8], F. Iemmi, C.H. Jiang, A. Kapoor, H. Liao, Z.-A. Liu[11], F. Monti, R. Sharma, J.N. Song, J. Tao, J. Wang, H. Zhang

State Key Laboratory of Nuclear Physics and Technology, Peking University, Beijing, China
A. Agapitos, Y. Ban, A. Levin, C. Li, Q. Li, X. Lyu, Y. Mao, S.J. Qian, X. Sun, D. Wang, H. Yang

Sun Yat-Sen University, Guangzhou, China
M. Lu, Z. You

University of Science and Technology of China, Hefei, China
N. Lu

Institute of Modern Physics and Key Laboratory of Nuclear Physics and Ion-beam Application (MOE) — Fudan University, Shanghai, China
X. Gao[4], D. Leggat, H. Okawa, Y. Zhang

Zhejiang University, Hangzhou, Zhejiang, China
Z. Lin, C. Lu, M. Xiao

Universidad de Los Andes, Bogota, Colombia
C. Avila, D.A. Barbosa Trujillo, A. Cabrera, C. Florez, J. Fraga, J.A. Reyes Vega

Universidad de Antioquia, Medellin, Colombia
J. Mejia Guisao, F. Ramirez, M. Rodriguez, J.D. Ruiz Alvarez

JHEP01(2025)011

University of Split, Faculty of Electrical Engineering, Mechanical Engineering and Naval Architecture, Split, Croatia
D. Giljanovic, N. Godinovic, D. Lelas, A. Sculac

University of Split, Faculty of Science, Split, Croatia
M. Kovac, T. Sculac

Institute Rudjer Boskovic, Zagreb, Croatia
P. Bargassa, V. Brigljevic, B.K. Chitroda, D. Ferencek, S. Mishra, A. Starodumov[12], T. Susa

University of Cyprus, Nicosia, Cyprus
A. Attikis, K. Christoforou, S. Konstantinou, J. Mousa, C. Nicolaou, F. Ptochos, P.A. Razis, H. Rykaczewski, H. Saka, A. Stepennov

Charles University, Prague, Czech Republic
M. Finger, M. Finger Jr., A. Kveton

Escuela Politecnica Nacional, Quito, Ecuador
E. Ayala

Universidad San Francisco de Quito, Quito, Ecuador
E. Carrera Jarrin

Academy of Scientific Research and Technology of the Arab Republic of Egypt, Egyptian Network of High Energy Physics, Cairo, Egypt
S. Elgammal[13], A. Ellithi Kamel[14]

Center for High Energy Physics (CHEP-FU), Fayoum University, El-Fayoum, Egypt
M.A. Mahmoud, Y. Mohammed

National Institute of Chemical Physics and Biophysics, Tallinn, Estonia
K. Ehataht, M. Kadastik, T. Lange, S. Nandan, C. Nielsen, J. Pata, M. Raidal, L. Tani, C. Veelken

Department of Physics, University of Helsinki, Helsinki, Finland
H. Kirschenmann, K. Osterberg, M. Voutilainen

Helsinki Institute of Physics, Helsinki, Finland
S. Bharthuar, E. Brücken, F. Garcia, J. Havukainen, M.S. Kim, R. Kinnunen, T. Lampén, K. Lassila-Perini, S. Lehti, T. Lindén, M. Lotti, L. Martikainen, M. Myllymäki, M.m. Rantanen, H. Siikonen, E. Tuominen, J. Tuominiemi

Lappeenranta-Lahti University of Technology, Lappeenranta, Finland
P. Luukka, H. Petrow, T. Tuuva†

JHEP01(2025)011

IRFU, CEA, Université Paris-Saclay, Gif-sur-Yvette, France
C. Amendola, M. Besancon, F. Couderc, M. Dejardin, D. Denegri, J.L. Faure, F. Ferri, S. Ganjour, P. Gras, G. Hamel de Monchenault, V. Lohezic, J. Malcles, J. Rander, A. Rosowsky, M.Ö. Sahin, A. Savoy-Navarro[15], P. Simkina, M. Titov

Laboratoire Leprince-Ringuet, CNRS/IN2P3, Ecole Polytechnique, Institut Polytechnique de Paris, Palaiseau, France
C. Baldenegro Barrera, F. Beaudette, A. Buchot Perraguin, P. Busson, A. Cappati, C. Charlot, F. Damas, O. Davignon, B. Diab, G. Falmagne, B.A. Fontana Santos Alves, S. Ghosh, R. Granier de Cassagnac, A. Hakimi, B. Harikrishnan, G. Liu, J. Motta, M. Nguyen, C. Ochando, L. Portales, R. Salerno, U. Sarkar, J.B. Sauvan, Y. Sirois, A. Tarabini, E. Vernazza, A. Zabi, A. Zghiche

Université de Strasbourg, CNRS, IPHC UMR 7178, Strasbourg, France
J.-L. Agram[16], J. Andrea, D. Apparu, D. Bloch, J.-M. Brom, E.C. Chabert, C. Collard, U. Goerlach, C. Grimault, A.-C. Le Bihan, P. Van Hove

Institut de Physique des 2 Infinis de Lyon (IP2I), Villeurbanne, France
S. Beauceron, B. Blancon, G. Boudoul, N. Chanon, J. Choi, D. Contardo, P. Depasse, C. Dozen[17], H. El Mamouni, J. Fay, S. Gascon, M. Gouzevitch, C. Greenberg, G. Grenier, B. Ille, I.B. Laktineh, M. Lethuillier, L. Mirabito, S. Perries, M. Vander Donckt, P. Verdier, J. Xiao

Georgian Technical University, Tbilisi, Georgia
I. Lomidze, T. Toriashvili[18], Z. Tsamalaidze[12]

RWTH Aachen University, I. Physikalisches Institut, Aachen, Germany
V. Botta, L. Feld, K. Klein, M. Lipinski, D. Meuser, A. Pauls, N. Röwert, M. Teroerde

RWTH Aachen University, III. Physikalisches Institut A, Aachen, Germany
S. Diekmann, A. Dodonova, N. Eich, D. Eliseev, M. Erdmann, P. Fackeldey, B. Fischer, T. Hebbeker, K. Hoepfner, F. Ivone, M.y. Lee, L. Mastrolorenzo, M. Merschmeyer, A. Meyer, S. Mondal, S. Mukherjee, D. Noll, A. Novak, F. Nowotny, A. Pozdnyakov, Y. Rath, W. Redjeb, F. Rehm, H. Reithler, A. Schmidt, S.C. Schuler, A. Sharma, A. Stein, F. Torres Da Silva De Araujo[19], L. Vigilante, S. Wiedenbeck, S. Zaleski

RWTH Aachen University, III. Physikalisches Institut B, Aachen, Germany
C. Dziwok, G. Flügge, W. Haj Ahmad[20], T. Kress, A. Nowack, O. Pooth, A. Stahl, T. Ziemons, A. Zotz

Deutsches Elektronen-Synchrotron, Hamburg, Germany
H. Aarup Petersen, M. Aldaya Martin, J. Alimena, S. Amoroso, Y. An, S. Baxter, M. Bayatmakou, H. Becerril Gonzalez, O. Behnke, S. Bhattacharya, F. Blekman[21], K. Borras[22], D. Brunner, A. Campbell, A. Cardini, C. Cheng, F. Colombina, S. Consuegra Rodríguez, G. Correia Silva, M. De Silva, G. Eckerlin, D. Eckstein,

JHEP01(2025)011

L.I. Estevez Banos, O. Filatov, E. Gallo[21], A. Geiser, A. Giraldi, G. Greau, A. Grohsjean, V. Guglielmi, M. Guthoff, A. Jafari[23], N.Z. Jomhari, B. Kaech, M. Kasemann, H. Kaveh, C. Kleinwort, R. Kogler, M. Komm, D. Krücker, W. Lange, D. Leyva Pernia, K. Lipka[24], W. Lohmann[25], R. Mankel, I.-A. Melzer-Pellmann, M. Mendizabal Morentin, J. Metwally, A.B. Meyer, G. Milella, M. Mormile, A. Mussgiller, A. Nürnberg, Y. Otarid, D. Pérez Adán, E. Ranken, A. Raspereza, B. Ribeiro Lopes, J. Rübenach, A. Saggio, M. Scham[26,22], V. Scheurer, S. Schnake[22], P. Schütze, C. Schwanenberger[21], M. Shchedrolosiev, R.E. Sosa Ricardo, L.P. Sreelatha Pramod, D. Stafford, F. Vazzoler, A. Ventura Barroso, R. Walsh, Q. Wang, Y. Wen, K. Wichmann, L. Wiens[22], C. Wissing, S. Wuchterl, Y. Yang, A. Zimermmane Castro Santos

University of Hamburg, Hamburg, Germany

A. Albrecht, S. Albrecht, M. Antonello, S. Bein, L. Benato, M. Bonanomi, P. Connor, K. De Leo, M. Eich, K. El Morabit, A. Fröhlich, C. Garbers, E. Garutti, M. Hajheidari, J. Haller, A. Hinzmann, H.R. Jabusch, G. Kasieczka, P. Keicher, R. Klanner, W. Korcari, T. Kramer, V. Kutzner, F. Labe, J. Lange, A. Lobanov, C. Matthies, A. Mehta, L. Moureaux, M. Mrowietz, A. Nigamova, Y. Nissan, A. Paasch, K.J. Pena Rodriguez, T. Quadfasel, M. Rieger, D. Savoiu, J. Schindler, P. Schleper, M. Schröder, J. Schwandt, M. Sommerhalder, H. Stadie, G. Steinbrück, A. Tews, M. Wolf

Karlsruher Institut fuer Technologie, Karlsruhe, Germany

S. Brommer, M. Burkart, E. Butz, T. Chwalek, A. Dierlamm, A. Droll, N. Faltermann, M. Giffels, A. Gottmann, F. Hartmann[27], M. Horzela, U. Husemann, M. Klute, R. Koppenhöfer, M. Link, A. Lintuluoto, S. Maier, S. Mitra, Th. Müller, M. Neukum, G. Quast, K. Rabbertz, I. Shvetsov, H.J. Simonis, N. Trevisani, R. Ulrich, J. van der Linden, M. Wassmer, S. Wieland, R. Wolf, S. Wunsch

Institute of Nuclear and Particle Physics (INPP), NCSR Demokritos, Aghia Paraskevi, Greece

G. Anagnostou, P. Assiouras, G. Daskalakis, A. Kyriakis, A. Stakia

National and Kapodistrian University of Athens, Athens, Greece

D. Karasavvas, P. Kontaxakis, G. Melachroinos, A. Panagiotou, I. Papavergou, I. Paraskevas, N. Saoulidou, K. Theofilatos, E. Tziaferi, K. Vellidis, I. Zisopoulos

National Technical University of Athens, Athens, Greece

G. Bakas, T. Chatzistavrou, G. Karapostoli, K. Kousouris, I. Papakrivopoulos, E. Siamarkou, G. Tsipolitis, A. Zacharopoulou

University of Ioánnina, Ioánnina, Greece

K. Adamidis, I. Bestintzanos, I. Evangelou, C. Foudas, P. Gianneios, C. Kamtsikis, P. Katsoulis, P. Kokkas, P.G. Kosmoglou Kioseoglou, N. Manthos, I. Papadopoulos, J. Strologas

HUN-REN Wigner Research Centre for Physics, Budapest, Hungary

M. Bartók[28], C. Hajdu, D. Horvath[29,30], F. Sikler, V. Veszpremi

JHEP01(2025)011

MTA-ELTE Lendület CMS Particle and Nuclear Physics Group, Eötvös Loránd University, Budapest, Hungary
M. Csanád, K. Farkas, M.M.A. Gadallah[31], P. Major, K. Mandal, G. Pásztor, A.J. Rádl[32], O. Surányi, G.I. Veres

Institute of Nuclear Research ATOMKI, Debrecen, Hungary
G. Bencze, S. Czellar, J. Karancsi[28], J. Molnar, Z. Szillasi

Institute of Physics, University of Debrecen, Debrecen, Hungary
P. Raics, B. Ujvari[33], G. Zilizi

Karoly Robert Campus, MATE Institute of Technology, Gyongyos, Hungary
T. Csorgo[32], F. Nemes[32], T. Novak

Panjab University, Chandigarh, India
J. Babbar, S. Bansal, S.B. Beri, V. Bhatnagar, G. Chaudhary, S. Chauhan, N. Dhingra[34], R. Gupta, A. Kaur, A. Kaur, H. Kaur, M. Kaur, S. Kumar, P. Kumari, M. Meena, K. Sandeep, T. Sheokand, J.B. Singh[35], A. Singla

University of Delhi, Delhi, India
A. Ahmed, A. Bhardwaj, A. Chhetri, B.C. Choudhary, A. Kumar, M. Naimuddin, K. Ranjan, S. Saumya

Saha Institute of Nuclear Physics, HBNI, Kolkata, India
S. Baradia, S. Barman[36], S. Bhattacharya, D. Bhowmik, S. Dutta, S. Dutta, B. Gomber[37], P. Palit, G. Saha, B. Sahu[37], S. Sarkar

Indian Institute of Technology Madras, Madras, India
P.K. Behera, S.C. Behera, S. Chatterjee, P. Jana, P. Kalbhor, J.R. Komaragiri[38], D. Kumar[38], M. Mohammad Mobassir Ameen, A. Muhammad, L. Panwar[38], R. Pradhan, P.R. Pujahari, N.R. Saha, A. Sharma, A.K. Sikdar, S. Verma

Tata Institute of Fundamental Research-A, Mumbai, India
T. Aziz, I. Das, S. Dugad, M. Kumar, G.B. Mohanty, P. Suryadevara

Tata Institute of Fundamental Research-B, Mumbai, India
A. Bala, S. Banerjee, M. Guchait, S. Karmakar, S. Kumar, G. Majumder, K. Mazumdar, S. Mukherjee, A. Thachayath

National Institute of Science Education and Research, An OCC of Homi Bhabha National Institute, Bhubaneswar, Odisha, India
S. Bahinipati[39], A.K. Das, C. Kar, D. Maity, P. Mal, T. Mishra, V.K. Muraleedharan Nair Bindhu[40], K. Naskar[40], A. Nayak[40], P. Saha, S.K. Swain, S. Varghese[40], D. Vats[40]

Indian Institute of Science Education and Research (IISER), Pune, India
A. Alpana, S. Dube, B. Kansal, A. Laha, S. Pandey, A. Rastogi, S. Sharma

Isfahan University of Technology, Isfahan, Iran
H. Bakhshiansohi[41,42], E. Khazaie[42], M. Zeinali[43]

Institute for Research in Fundamental Sciences (IPM), Tehran, Iran
S. Chenarani[44], S.M. Etesami, M. Khakzad, M. Mohammadi Najafabadi

University College Dublin, Dublin, Ireland
M. Grunewald

INFN Sezione di Bari[a], Università di Bari[b], Politecnico di Bari[c], Bari, Italy
M. Abbrescia[a,b], R. Aly[a,b,45], C. Aruta[a,b], A. Colaleo[a], D. Creanza[a,c], B. D'Anzi[a,b], N. De Filippis[a,c], M. De Palma[a,b], A. Di Florio[a,b], W. Elmetenawee[a,b], F. Errico[a,b], L. Fiore[a], G. Iaselli[a,c], G. Maggi[a,c], M. Maggi[a], I. Margjeka[a,b], V. Mastrapasqua[a,b], S. My[a,b], S. Nuzzo[a,b], A. Pellecchia[a,b], A. Pompili[a,b], G. Pugliese[a,c], R. Radogna[a], D. Ramos[a], A. Ranieri[a], G. Selvaggi[a,b], L. Silvestris[a], F.M. Simone[a,b], Ü. Sözbilir[a], A. Stamerra[a], R. Venditti[a], P. Verwilligen[a]

INFN Sezione di Bologna[a], Università di Bologna[b], Bologna, Italy
G. Abbiendi[a], C. Battilana[a,b], L. Borgonovi[a], L. Brigliadori[a], P. Capiluppi[a,b], A. Castro[a,b], F.R. Cavallo[a], M. Cuffiani[a,b], G.M. Dallavalle[a], T. Diotalevi[a,b], F. Fabbri[a], A. Fanfani[a,b], D. Fasanella[a,b], P. Giacomelli[a], L. Giommi[a,b], C. Grandi[a], L. Guiducci[a,b], S. Lo Meo[a,46], L. Lunerti[a,b], S. Marcellini[a], G. Masetti[a], F.L. Navarria[a,b], A. Perrotta[a], F. Primavera[a,b], A.M. Rossi[a,b], T. Rovelli[a,b], G.P. Siroli[a,b]

INFN Sezione di Catania[a], Università di Catania[b], Catania, Italy
S. Costa[a,b,47], A. Di Mattia[a], R. Potenza[a,b], A. Tricomi[a,b,47], C. Tuve[a,b]

INFN Sezione di Firenze[a], Università di Firenze[b], Firenze, Italy
G. Barbagli[a], G. Bardelli[a,b], B. Camaiani[a,b], A. Cassese[a], R. Ceccarelli[a,b], V. Ciulli[a,b], C. Civinini[a], R. D'Alessandro[a,b], E. Focardi[a,b], G. Latino[a,b], P. Lenzi[a,b], M. Lizzo[a,b], M. Meschini[a], S. Paoletti[a], G. Sguazzoni[a], L. Viliani[a]

INFN Laboratori Nazionali di Frascati, Frascati, Italy
L. Benussi, S. Bianco, S. Meola[48], D. Piccolo

INFN Sezione di Genova[a], Università di Genova[b], Genova, Italy
P. Chatagnon[a], F. Ferro[a], E. Robutti[a], S. Tosi[a,b]

INFN Sezione di Milano-Bicocca[a], Università di Milano-Bicocca[b], Milano, Italy
A. Benaglia[a], G. Boldrini[a], F. Brivio[a,b], F. Cetorelli[a,b], F. De Guio[a,b], M.E. Dinardo[a,b], P. Dini[a], S. Gennai[a], A. Ghezzi[a,b], P. Govoni[a,b], L. Guzzi[a,b], M.T. Lucchini[a,b], M. Malberti[a], S. Malvezzi[a], A. Massironi[a], D. Menasce[a], L. Moroni[a], M. Paganoni[a,b], D. Pedrini[a], B.S. Pinolini[a], S. Ragazzi[a,b], N. Redaelli[a], T. Tabarelli de Fatis[a,b], D. Zuolo[a,b]

JHEP01(2025)011

INFN Sezione di Napoli[a], Università di Napoli 'Federico II'[b], Napoli, Italy; Università della Basilicata[c], Potenza, Italy; Scuola Superiore Meridionale (SSM)[d], Napoli, Italy

S. Buontempo[a], A. Cagnotta[a,b], F. Carnevali[a,b], N. Cavallo[a,c], A. De Iorio[a,b], F. Fabozzi[a,c], A.O.M. Iorio[a,b], L. Lista[a,b,49], P. Paolucci[a,27], B. Rossi[a], C. Sciacca[a,b]

INFN Sezione di Padova[a], Università di Padova[b], Padova, Italy; Università di Trento[c], Trento, Italy

R. Ardino[a], P. Azzi[a], N. Bacchetta[a,50], D. Bisello[a,b], P. Bortignon[a], A. Bragagnolo[a,b], R. Carlin[a,b], T. Dorigo[a], F. Gasparini[a,b], U. Gasparini[a,b], G. Govi[a], A. Gozzelino[a], G. Grosso[a], L. Layer[a,51], E. Lusiani[a], M. Margoni[a,b], A.T. Meneguzzo[a,b], M. Migliorini[a,b], J. Pazzini[a,b], P. Ronchese[a,b], R. Rossin[a,b], F. Simonetto[a,b], G. Strong[a], M. Tosi[a,b], A. Triossi[a,b], S. Ventura[a], H. Yarar[a,b], M. Zanetti[a,b], P. Zotto[a,b], A. Zucchetta[a,b]

INFN Sezione di Pavia[a], Università di Pavia[b], Pavia, Italy

S. Abu Zeid[a,52], C. Aimè[a,b], A. Braghieri[a], S. Calzaferri[a,b], D. Fiorina[a,b], P. Montagna[a,b], V. Re[a], C. Riccardi[a,b], P. Salvini[a], I. Vai[a,b], P. Vitulo[a,b]

INFN Sezione di Perugia[a], Università di Perugia[b], Perugia, Italy

P. Asenov[a,53], G.M. Bilei[a], D. Ciangottini[a,b], L. Fanò[a,b], M. Magherini[a,b], G. Mantovani[a,b], V. Mariani[a,b], M. Menichelli[a], F. Moscatelli[a,53], A. Piccinelli[a,b], M. Presilla[a,b], A. Rossi[a,b], A. Santocchia[a,b], D. Spiga[a], T. Tedeschi[a,b]

INFN Sezione di Pisa[a], Università di Pisa[b], Scuola Normale Superiore di Pisa[c], Pisa, Italy; Università di Siena[d], Siena, Italy

P. Azzurri[a], G. Bagliesi[a], R. Bhattacharya[a], L. Bianchini[a,b], T. Boccali[a], E. Bossini[a,b], D. Bruschini[a,c], R. Castaldi[a], M.A. Ciocci[a,b], V. D'Amante[a,d], R. Dell'Orso[a], S. Donato[a], A. Giassi[a], F. Ligabue[a,c], D. Matos Figueiredo[a], A. Messineo[a,b], M. Musich[a,b], F. Palla[a], S. Parolia[a], G. Ramirez-Sanchez[a,c], A. Rizzi[a,b], G. Rolandi[a,c], S. Roy Chowdhury[a], T. Sarkar[a], A. Scribano[a], P. Spagnolo[a], R. Tenchini[a], G. Tonelli[a,b], N. Turini[a,d], A. Venturi[a], P.G. Verdini[a]

INFN Sezione di Roma[a], Sapienza Università di Roma[b], Roma, Italy

P. Barria[a], M. Campana[a,b], F. Cavallari[a], L. Cunqueiro Mendez[a,b], D. Del Re[a,b], E. Di Marco[a], M. Diemoz[a], E. Longo[a,b], P. Meridiani[a], J. Mijuskovic[a,b,54], G. Organtini[a,b], F. Pandolfi[a], R. Paramatti[a,b], C. Quaranta[a,b], S. Rahatlou[a,b], C. Rovelli[a], F. Santanastasio[a,b], L. Soffi[a], R. Tramontano[a,b]

INFN Sezione di Torino[a], Università di Torino[b], Torino, Italy; Università del Piemonte Orientale[c], Novara, Italy

N. Amapane[a,b], R. Arcidiacono[a,c], S. Argiro[a,b], M. Arneodo[a,c], N. Bartosik[a], R. Bellan[a,b], A. Bellora[a,b], C. Biino[a], N. Cartiglia[a], M. Costa[a,b], R. Covarelli[a,b], N. Demaria[a], L. Finco[a], M. Grippo[a,b], B. Kiani[a,b], F. Legger[a], F. Luongo[a,b], C. Mariotti[a], S. Maselli[a], A. Mecca[a,b], E. Migliore[a,b], M. Monteno[a], R. Mulargia[a], M.M. Obertino[a,b], G. Ortona[a], L. Pacher[a,b], N. Pastrone[a], M. Pelliccioni[a], M. Ruspa[a,c],

K. Shchelina[a], F. Siviero[a,b], V. Sola[a,b], A. Solano[a,b], D. Soldi[a,b], A. Staiano[a], C. Tarricone[a,b], M. Tornago[a,b], D. Trocino[a], G. Umoret[a,b], A. Vagnerini[a,b], E. Vlasov[a,b]

INFN Sezione di Trieste[a], Università di Trieste[b], Trieste, Italy
S. Belforte[a], V. Candelise[a,b], M. Casarsa[a], F. Cossutti[a], G. Della Ricca[a,b], G. Sorrentino[a,b]

Kyungpook National University, Daegu, Korea
S. Dogra, C. Huh, B. Kim, D.H. Kim, J. Kim, J. Lee, S.W. Lee, C.S. Moon, Y.D. Oh, S.I. Pak, M.S. Ryu, S. Sekmen, Y.C. Yang

Chonnam National University, Institute for Universe and Elementary Particles, Kwangju, Korea
H. Kim, D.H. Moon

Hanyang University, Seoul, Korea
E. Asilar, T.J. Kim, J. Park

Korea University, Seoul, Korea
S. Choi, S. Han, B. Hong, K. Lee, K.S. Lee, J. Lim, J. Park, S.K. Park, J. Yoo

Kyung Hee University, Department of Physics, Seoul, Korea
J. Goh

Sejong University, Seoul, Korea
H. S. Kim, Y. Kim, S. Lee

Seoul National University, Seoul, Korea
J. Almond, J.H. Bhyun, J. Choi, S. Jeon, J. Kim, J.S. Kim, S. Ko, H. Kwon, H. Lee, S. Lee, B.H. Oh, S.B. Oh, H. Seo, U.K. Yang, I. Yoon

University of Seoul, Seoul, Korea
W. Jang, D.Y. Kang, Y. Kang, D. Kim, S. Kim, B. Ko, J.S.H. Lee, Y. Lee, J.A. Merlin, I.C. Park, Y. Roh, I.J. Watson, S. Yang

Yonsei University, Department of Physics, Seoul, Korea
S. Ha, H.D. Yoo

Sungkyunkwan University, Suwon, Korea
M. Choi, M.R. Kim, H. Lee, Y. Lee, I. Yu

College of Engineering and Technology, American University of the Middle East (AUM), Dasman, Kuwait
T. Beyrouthy, Y. Maghrbi

Riga Technical University, Riga, Latvia
K. Dreimanis, A. Gaile, G. Pikurs, A. Potrebko, M. Seidel, V. Veckalns[55]

University of Latvia (LU), Riga, Latvia
N.R. Strautnieks

Vilnius University, Vilnius, Lithuania
M. Ambrozas, A. Juodagalvis, A. Rinkevicius, G. Tamulaitis

National Centre for Particle Physics, Universiti Malaya, Kuala Lumpur, Malaysia
N. Bin Norjoharuddeen, I. Yusuff[56], Z. Zolkapli

Universidad de Sonora (UNISON), Hermosillo, Mexico
J.F. Benitez, A. Castaneda Hernandez, H.A. Encinas Acosta, L.G. Gallegos Maríñez, M. León Coello, J.A. Murillo Quijada, A. Sehrawat, L. Valencia Palomo

Centro de Investigacion y de Estudios Avanzados del IPN, Mexico City, Mexico
G. Ayala, H. Castilla-Valdez, E. De La Cruz-Burelo, I. Heredia-De La Cruz[57], R. Lopez-Fernandez, C.A. Mondragon Herrera, D.A. Perez Navarro, A. Sánchez Hernández

Universidad Iberoamericana, Mexico City, Mexico
C. Oropeza Barrera, M. Ramírez García

Benemerita Universidad Autonoma de Puebla, Puebla, Mexico
I. Pedraza, H.A. Salazar Ibarguen, C. Uribe Estrada

University of Montenegro, Podgorica, Montenegro
I. Bubanja, N. Raicevic

University of Canterbury, Christchurch, New Zealand
P.H. Butler

National Centre for Physics, Quaid-I-Azam University, Islamabad, Pakistan
A. Ahmad, M.I. Asghar, A. Awais, M.I.M. Awan, H.R. Hoorani, W.A. Khan

AGH University of Krakow, Faculty of Computer Science, Electronics and Telecommunications, Krakow, Poland
V. Avati, L. Grzanka, M. Malawski

National Centre for Nuclear Research, Swierk, Poland
H. Bialkowska, M. Bluj, B. Boimska, M. Górski, M. Kazana, M. Szleper, P. Zalewski

Institute of Experimental Physics, Faculty of Physics, University of Warsaw, Warsaw, Poland
K. Bunkowski, K. Doroba, A. Kalinowski, M. Konecki, J. Krolikowski

Warsaw University of Technology, Warsaw, Poland
K. Pozniak, W. Zabolotny

JHEP01(2025)011

Laboratório de Instrumentação e Física Experimental de Partículas, Lisboa, Portugal
M. Araujo, D. Bastos, C. Beirão Da Cruz E Silva, A. Boletti, M. Bozzo, P. Faccioli, M. Gallinaro, J. Hollar, N. Leonardo, T. Niknejad, M. Pisano, J. Seixas, J. Varela

Faculty of Physics, University of Belgrade, Belgrade, Serbia
P. Adzic, P. Milenovic

VINCA Institute of Nuclear Sciences, University of Belgrade, Belgrade, Serbia
M. Dordevic, J. Milosevic, V. Rekovic

Centro de Investigaciones Energéticas Medioambientales y Tecnológicas (CIEMAT), Madrid, Spain
M. Aguilar-Benitez, J. Alcaraz Maestre, M. Barrio Luna, Cristina F. Bedoya, M. Cepeda, M. Cerrada, N. Colino, B. De La Cruz, A. Delgado Peris, D. Fernández Del Val, J.P. Fernández Ramos, J. Flix, M.C. Fouz, O. Gonzalez Lopez, S. Goy Lopez, J.M. Hernandez, M.I. Josa, J. León Holgado, D. Moran, Á. Navarro Tobar, C. Perez Dengra, A. Pérez-Calero Yzquierdo, J. Puerta Pelayo, I. Redondo, D.D. Redondo Ferrero, L. Romero, S. Sánchez Navas, L. Urda Gómez, J. Vazquez Escobar, C. Willmott

Universidad Autónoma de Madrid, Madrid, Spain
J.F. de Trocóniz

Universidad de Oviedo, Instituto Universitario de Ciencias y Tecnologías Espaciales de Asturias (ICTEA), Oviedo, Spain
B. Alvarez Gonzalez, J. Cuevas, J. Fernandez Menendez, S. Folgueras, I. Gonzalez Caballero, J.R. González Fernández, E. Palencia Cortezon, C. Ramón Álvarez, V. Rodríguez Bouza, A. Soto Rodríguez, A. Trapote, C. Vico Villalba

Instituto de Física de Cantabria (IFCA), CSIC-Universidad de Cantabria, Santander, Spain
S. Bhowmik, S. Blanco Fernández, J.A. Brochero Cifuentes, I.J. Cabrillo, A. Calderon, J. Duarte Campderros, M. Fernandez, C. Fernandez Madrazo, G. Gomez, C. Lasaosa García, C. Martinez Rivero, P. Martinez Ruiz del Arbol, F. Matorras, P. Matorras Cuevas, E. Navarrete Ramos, J. Piedra Gomez, C. Prieels, L. Scodellaro, I. Vila, J.M. Vizan Garcia

University of Colombo, Colombo, Sri Lanka
M.K. Jayananda, B. Kailasapathy[58], D.U.J. Sonnadara, D.D.C. Wickramarathna

University of Ruhuna, Department of Physics, Matara, Sri Lanka
W.G.D. Dharmaratna, K. Liyanage, N. Perera, N. Wickramage

CERN, European Organization for Nuclear Research, Geneva, Switzerland
D. Abbaneo, E. Auffray, G. Auzinger, J. Baechler, D. Barney, A. Bermúdez Martínez, M. Bianco, B. Bilin, A.A. Bin Anuar, A. Bocci, E. Brondolin, C. Caillol,

T. Camporesi, G. Cerminara, N. Chernyavskaya, M. Cipriani, D. d'Enterria, A. Dabrowski, A. David, A. De Roeck, M.M. Defranchis, M. Deile, M. Dobson, F. Fallavollita[59], L. Forthomme, G. Franzoni, W. Funk, S. Giani, D. Gigi, K. Gill, F. Glege, L. Gouskos, M. Haranko, J. Hegeman, T. James, J. Kieseler, N. Kratochwil, S. Laurila, P. Lecoq, E. Leutgeb, C. Lourenço, B. Maier, L. Malgeri, M. Mannelli, A.C. Marini, F. Meijers, S. Mersi, E. Meschi, F. Moortgat, M. Mulders, S. Orfanelli, F. Pantaleo, M. Peruzzi, A. Petrilli, G. Petrucciani, A. Pfeiffer, M. Pierini, D. Piparo, H. Qu, D. Rabady, G. Reales Gutiérrez, M. Rovere, H. Sakulin, S. Scarfi, M. Selvaggi, A. Sharma, P. Silva, P. Sphicas[60], A.G. Stahl Leiton, A. Steen, S. Summers, D. Treille, P. Tropea, A. Tsirou, D. Walter, J. Wanczyk[61], K.A. Wozniak, P. Zejdl, W.D. Zeuner

Paul Scherrer Institut, Villigen, Switzerland

T. Bevilacqua[62], L. Caminada[62], A. Ebrahimi, W. Erdmann, R. Horisberger, Q. Ingram, H.C. Kaestli, D. Kotlinski, C. Lange, M. Missiroli[62], L. Noehte[62], T. Rohe

ETH Zurich — Institute for Particle Physics and Astrophysics (IPA), Zurich, Switzerland

T.K. Aarrestad, K. Androsov[61], M. Backhaus, A. Calandri, K. Datta, A. De Cosa, G. Dissertori, M. Dittmar, M. Donegà, F. Eble, M. Galli, K. Gedia, F. Glessgen, C. Grab, D. Hits, W. Lustermann, A.-M. Lyon, R.A. Manzoni, L. Marchese, C. Martin Perez, A. Mascellani[61], F. Nessi-Tedaldi, F. Pauss, V. Perovic, S. Pigazzini, M.G. Ratti, M. Reichmann, C. Reissel, T. Reitenspiess, B. Ristic, F. Riti, D. Ruini, D.A. Sanz Becerra, R. Seidita, J. Steggemann[61], D. Valsecchi, R. Wallny

Universität Zürich, Zurich, Switzerland

C. Amsler[63], P. Bärtschi, C. Botta, D. Brzhechko, M.F. Canelli, K. Cormier, A. De Wit, R. Del Burgo, J.K. Heikkilä, M. Huwiler, W. Jin, A. Jofrehei, B. Kilminster, S. Leontsinis, S.P. Liechti, A. Macchiolo, P. Meiring, V.M. Mikuni, U. Molinatti, I. Neutelings, A. Reimers, P. Robmann, S. Sanchez Cruz, K. Schweiger, M. Senger, Y. Takahashi

National Central University, Chung-Li, Taiwan

C. Adloff[64], C.M. Kuo, W. Lin, P.K. Rout, P.C. Tiwari[38], S.S. Yu

National Taiwan University (NTU), Taipei, Taiwan

L. Ceard, Y. Chao, K.F. Chen, P.s. Chen, W.-S. Hou, Y.w. Kao, R. Khurana, G. Kole, Y.y. Li, R.-S. Lu, E. Paganis, A. Psallidas, J. Thomas-Wilsker, H.y. Wu, E. Yazgan

High Energy Physics Research Unit, Department of Physics, Faculty of Science, Chulalongkorn University, Bangkok, Thailand

C. Asawatangtrakuldee, N. Srimanobhas, V. Wachirapusitanand

Çukurova University, Physics Department, Science and Art Faculty, Adana, Turkey

D. Agyel, F. Boran, Z.S. Demiroglu, F. Dolek, I. Dumanoglu[65], E. Eskut, Y. Guler[66],

JHEP01(2025)011

E. Gurpinar Guler[66], C. Isik, O. Kara, A. Kayis Topaksu, U. Kiminsu, G. Onengut, K. Ozdemir[67], A. Polatoz, B. Tali[68], U.G. Tok, S. Turkcapar, E. Uslan, I.S. Zorbakir

Middle East Technical University, Physics Department, Ankara, Turkey
K. Ocalan[69], M. Yalvac[70]

Bogazici University, Istanbul, Turkey
B. Akgun, I.O. Atakisi, E. Gülmez, M. Kaya[71], O. Kaya[72], S. Tekten[73]

Istanbul Technical University, Istanbul, Turkey
A. Cakir, K. Cankocak[65], Y. Komurcu, S. Sen[74]

Istanbul University, Istanbul, Turkey
O. Aydilek, S. Cerci[68], V. Epshteyn, B. Hacisahinoglu, I. Hos[75], B. Isildak[76], B. Kaynak, S. Ozkorucuklu, H. Sert, C. Simsek, D. Sunar Cerci[68], C. Zorbilmez

Institute for Scintillation Materials of National Academy of Science of Ukraine, Kharkiv, Ukraine
A. Boyaryntsev, B. Grynyov

National Science Centre, Kharkiv Institute of Physics and Technology, Kharkiv, Ukraine
L. Levchuk

University of Bristol, Bristol, United Kingdom
D. Anthony, J.J. Brooke, A. Bundock, E. Clement, D. Cussans, H. Flacher, M. Glowacki, J. Goldstein, H.F. Heath, L. Kreczko, B. Krikler, S. Paramesvaran, S. Seif El Nasr-Storey, V.J. Smith, N. Stylianou[77], K. Walkingshaw Pass, R. White

Rutherford Appleton Laboratory, Didcot, United Kingdom
A.H. Ball, K.W. Bell, A. Belyaev[78], C. Brew, R.M. Brown, D.J.A. Cockerill, C. Cooke, K.V. Ellis, K. Harder, S. Harper, M.-L. Holmberg[79], Sh. Jain, J. Linacre, K. Manolopoulos, D.M. Newbold, E. Olaiya, D. Petyt, T. Reis, G. Salvi, T. Schuh, C.H. Shepherd-Themistocleous, I.R. Tomalin, T. Williams

Imperial College, London, United Kingdom
R. Bainbridge, P. Bloch, C.E. Brown, O. Buchmuller, V. Cacchio, C.A. Carrillo Montoya, V. Cepaitis, G.S. Chahal[80], D. Colling, J.S. Dancu, P. Dauncey, G. Davies, J. Davies, M. Della Negra, S. Fayer, G. Fedi, G. Hall, M.H. Hassanshahi, A. Howard, G. Iles, J. Langford, L. Lyons, A.-M. Magnan, S. Malik, A. Martelli, M. Mieskolainen, J. Nash[81], M. Pesaresi, B.C. Radburn-Smith, A. Richards, A. Rose, C. Seez, R. Shukla, A. Tapper, K. Uchida, G.P. Uttley, L.H. Vage, T. Virdee[27], M. Vojinovic, N. Wardle, D. Winterbottom

Brunel University, Uxbridge, United Kingdom
K. Coldham, J.E. Cole, A. Khan, P. Kyberd, I.D. Reid

JHEP01(2025)011

Baylor University, Waco, Texas, U.S.A.
S. Abdullin, A. Brinkerhoff, B. Caraway, J. Dittmann, K. Hatakeyama, J. Hiltbrand, A.R. Kanuganti, B. McMaster, M. Saunders, S. Sawant, C. Sutantawibul, M. Toms, J. Wilson

Catholic University of America, Washington, DC, U.S.A.
R. Bartek, A. Dominguez, C. Huerta Escamilla, A.E. Simsek, R. Uniyal, A.M. Vargas Hernandez

The University of Alabama, Tuscaloosa, Alabama, U.S.A.
R. Chudasama, S.I. Cooper, S.V. Gleyzer, C.U. Perez, P. Rumerio[82], E. Usai, C. West

Boston University, Boston, Massachusetts, U.S.A.
A. Akpinar, A. Albert, D. Arcaro, C. Cosby, Z. Demiragli, C. Erice, E. Fontanesi, D. Gastler, J. Rohlf, K. Salyer, D. Sperka, D. Spitzbart, I. Suarez, A. Tsatsos, S. Yuan

Brown University, Providence, Rhode Island, U.S.A.
G. Benelli, X. Coubez[22], D. Cutts, M. Hadley, U. Heintz, J.M. Hogan[83], T. Kwon, G. Landsberg, K.T. Lau, D. Li, J. Luo, M. Narain, N. Pervan, S. Sagir[84], F. Simpson, W.Y. Wong, X. Yan, D. Yu, W. Zhang

University of California, Davis, Davis, California, U.S.A.
S. Abbott, J. Bonilla, C. Brainerd, R. Breedon, M. Calderon De La Barca Sanchez, M. Chertok, J. Conway, P.T. Cox, R. Erbacher, G. Haza, F. Jensen, O. Kukral, G. Mocellin, M. Mulhearn, D. Pellett, B. Regnery, W. Wei, Y. Yao, F. Zhang

University of California, Los Angeles, California, U.S.A.
M. Bachtis, R. Cousins, A. Datta, J. Hauser, M. Ignatenko, M.A. Iqbal, T. Lam, E. Manca, W.A. Nash, D. Saltzberg, B. Stone, V. Valuev

University of California, Riverside, Riverside, California, U.S.A.
R. Clare, M. Gordon, G. Hanson, W. Si

University of California, San Diego, La Jolla, California, U.S.A.
J.G. Branson, S. Cittolin, S. Cooperstein, D. Diaz, J. Duarte, R. Gerosa, L. Giannini, J. Guiang, R. Kansal, V. Krutelyov, R. Lee, J. Letts, M. Masciovecchio, F. Mokhtar, M. Pieri, M. Quinnan, B.V. Sathia Narayanan, V. Sharma, M. Tadel, E. Vourliotis, F. Würthwein, Y. Xiang, A. Yagil

University of California, Santa Barbara — Department of Physics, Santa Barbara, California, U.S.A.
L. Brennan, C. Campagnari, M. Citron, G. Collura, A. Dorsett, J. Incandela, M. Kilpatrick, J. Kim, A.J. Li, P. Masterson, H. Mei, M. Oshiro, J. Richman, U. Sarica, R. Schmitz, F. Setti, J. Sheplock, D. Stuart, S. Wang

JHEP01(2025)011

California Institute of Technology, Pasadena, California, U.S.A.
A. Bornheim, O. Cerri, A. Latorre, J.M. Lawhorn, J. Mao, H.B. Newman, T. Q. Nguyen, M. Spiropulu, J.R. Vlimant, C. Wang, S. Xie, R.Y. Zhu

Carnegie Mellon University, Pittsburgh, Pennsylvania, U.S.A.
J. Alison, S. An, M.B. Andrews, P. Bryant, V. Dutta, T. Ferguson, A. Harilal, C. Liu, T. Mudholkar, S. Murthy, M. Paulini, A. Roberts, A. Sanchez, W. Terrill

University of Colorado Boulder, Boulder, Colorado, U.S.A.
J.P. Cumalat, W.T. Ford, A. Hassani, G. Karathanasis, E. MacDonald, N. Manganelli, F. Marini, A. Perloff, C. Savard, N. Schonbeck, K. Stenson, K.A. Ulmer, S.R. Wagner, N. Zipper

Cornell University, Ithaca, New York, U.S.A.
J. Alexander, S. Bright-Thonney, X. Chen, D.J. Cranshaw, J. Fan, X. Fan, D. Gadkari, S. Hogan, J. Monroy, J.R. Patterson, J. Reichert, M. Reid, A. Ryd, J. Thom, P. Wittich, R. Zou

Fermi National Accelerator Laboratory, Batavia, Illinois, U.S.A.
M. Albrow, M. Alyari, O. Amram, G. Apollinari, A. Apresyan, L.A.T. Bauerdick, D. Berry, J. Berryhill, P.C. Bhat, K. Burkett, J.N. Butler, A. Canepa, G.B. Cerati, H.W.K. Cheung, F. Chlebana, G. Cummings, J. Dickinson, I. Dutta, V.D. Elvira, Y. Feng, J. Freeman, A. Gandrakota, Z. Gecse, L. Gray, D. Green, S. Grünendahl, D. Guerrero, O. Gutsche, R.M. Harris, R. Heller, T.C. Herwig, J. Hirschauer, L. Horyn, B. Jayatilaka, S. Jindariani, M. Johnson, U. Joshi, T. Klijnsma, B. Klima, K.H.M. Kwok, S. Lammel, D. Lincoln, R. Lipton, T. Liu, C. Madrid, K. Maeshima, C. Mantilla, D. Mason, P. McBride, P. Merkel, S. Mrenna, S. Nahn, J. Ngadiuba, D. Noonan, V. Papadimitriou, N. Pastika, K. Pedro, C. Pena[85], F. Ravera, A. Reinsvold Hall[86], L. Ristori, E. Sexton-Kennedy, N. Smith, A. Soha, L. Spiegel, S. Stoynev, J. Strait, L. Taylor, S. Tkaczyk, N.V. Tran, L. Uplegger, E.W. Vaandering, I. Zoi

University of Florida, Gainesville, Florida, U.S.A.
P. Avery, D. Bourilkov, L. Cadamuro, P. Chang, V. Cherepanov, R.D. Field, E. Koenig, M. Kolosova, J. Konigsberg, A. Korytov, K.H. Lo, K. Matchev, N. Menendez, G. Mitselmakher, A. Muthirakalayil Madhu, N. Rawal, D. Rosenzweig, S. Rosenzweig, K. Shi, J. Wang

Florida State University, Tallahassee, Florida, U.S.A.
T. Adams, A. Al Kadhim, A. Askew, N. Bower, R. Habibullah, V. Hagopian, R. Hashmi, T. Kolberg, G. Martinez, H. Prosper, P.R. Prova, O. Viazlo, M. Wulansatiti, R. Yohay, J. Zhang

Florida Institute of Technology, Melbourne, Florida, U.S.A.
B. Alsufyani, M.M. Baarmand, S. Butalla, T. Elkafrawy[52], M. Hohlmann, R. Kumar Verma, M. Rahmani, F. Yumiceva

University of Illinois Chicago, Chicago, U.S.A., Chicago, U.S.A.
M.R. Adams, C. Bennett, R. Cavanaugh, S. Dittmer, O. Evdokimov, C.E. Gerber, D.J. Hofman, J.h. Lee, D. S. Lemos, A.H. Merrit, C. Mills, S. Nanda, G. Oh, D. Pilipovic, T. Roy, S. Rudrabhatla, M.B. Tonjes, N. Varelas, X. Wang, Z. Ye, J. Yoo

The University of Iowa, Iowa City, Iowa, U.S.A.
M. Alhusseini, D. Blend, K. Dilsiz[87], L. Emediato, G. Karaman, O.K. Köseyan, J.-P. Merlo, A. Mestvirishvili[88], J. Nachtman, O. Neogi, H. Ogul[89], Y. Onel, A. Penzo, C. Snyder, E. Tiras[90]

Johns Hopkins University, Baltimore, Maryland, U.S.A.
B. Blumenfeld, L. Corcodilos, J. Davis, A.V. Gritsan, L. Kang, S. Kyriacou, P. Maksimovic, M. Roguljic, J. Roskes, S. Sekhar, M. Swartz, T.Á. Vámi

The University of Kansas, Lawrence, Kansas, U.S.A.
A. Abreu, L.F. Alcerro Alcerro, J. Anguiano, P. Baringer, A. Bean, Z. Flowers, J. King, G. Krintiras, M. Lazarovits, C. Le Mahieu, C. Lindsey, J. Marquez, N. Minafra, M. Murray, M. Nickel, M. Pitt, S. Popescu[91], C. Rogan, C. Royon, R. Salvatico, S. Sanders, C. Smith, Q. Wang, G. Wilson

Kansas State University, Manhattan, Kansas, U.S.A.
B. Allmond, S. Duric, A. Ivanov, K. Kaadze, A. Kalogeropoulos, D. Kim, Y. Maravin, T. Mitchell, K. Nam, J. Natoli, D. Roy

Lawrence Livermore National Laboratory, Livermore, California, U.S.A.
F. Rebassoo, D. Wright

University of Maryland, College Park, Maryland, U.S.A.
E. Adams, A. Baden, O. Baron, A. Belloni, A. Bethani, Y.m. Chen, S.C. Eno, N.J. Hadley, S. Jabeen, R.G. Kellogg, T. Koeth, Y. Lai, S. Lascio, A.C. Mignerey, S. Nabili, C. Palmer, C. Papageorgakis, L. Wang, K. Wong

Massachusetts Institute of Technology, Cambridge, Massachusetts, U.S.A.
J. Bendavid, W. Busza, I.A. Cali, Y. Chen, M. D'Alfonso, J. Eysermans, C. Freer, G. Gomez-Ceballos, M. Goncharov, P. Harris, D. Hoang, D. Kovalskyi, J. Krupa, L. Lavezzo, Y.-J. Lee, K. Long, C. Mironov, C. Paus, C. Roland, G. Roland, S. Rothman, Z. Shi, G.S.F. Stephans, J. Wang, Z. Wang, B. Wyslouch, T. J. Yang

University of Minnesota, Minneapolis, Minnesota, U.S.A.
R.M. Chatterjee, B. Crossman, B.M. Joshi, C. Kapsiak, M. Krohn, D. Mahon, J. Mans, M. Revering, R. Rusack, R. Saradhy, N. Schroeder, N. Strobbe, M.A. Wadud

University of Mississippi, Oxford, Mississippi, U.S.A.
L.M. Cremaldi

University of Nebraska-Lincoln, Lincoln, Nebraska, U.S.A.
K. Bloom, M. Bryson, D.R. Claes, C. Fangmeier, F. Golf, C. Joo, I. Kravchenko, I. Reed, J.E. Siado, G.R. Snow[†], W. Tabb, A. Wightman, F. Yan, A.G. Zecchinelli

State University of New York at Buffalo, Buffalo, New York, U.S.A.
G. Agarwal, H. Bandyopadhyay, L. Hay, I. Iashvili, A. Kharchilava, C. McLean, M. Morris, D. Nguyen, J. Pekkanen, S. Rappoccio, H. Rejeb Sfar, A. Williams

Northeastern University, Boston, Massachusetts, U.S.A.
G. Alverson, E. Barberis, Y. Haddad, Y. Han, A. Krishna, J. Li, G. Madigan, B. Marzocchi, D.M. Morse, V. Nguyen, T. Orimoto, A. Parker, L. Skinnari, A. Tishelman-Charny, B. Wang, D. Wood

Northwestern University, Evanston, Illinois, U.S.A.
S. Bhattacharya, J. Bueghly, Z. Chen, A. Gilbert, K.A. Hahn, Y. Liu, D.G. Monk, M.H. Schmitt, A. Taliercio, M. Velasco

University of Notre Dame, Notre Dame, Indiana, U.S.A.
R. Band, R. Bucci, M. Cremonesi, A. Das, R. Goldouzian, M. Hildreth, K. Hurtado Anampa, C. Jessop, K. Lannon, J. Lawrence, N. Loukas, L. Lutton, J. Mariano, N. Marinelli, I. Mcalister, T. McCauley, C. Mcgrady, K. Mohrman, C. Moore, Y. Musienko[12], H. Nelson, R. Ruchti, A. Townsend, M. Wayne, H. Yockey, M. Zarucki, L. Zygala

The Ohio State University, Columbus, Ohio, U.S.A.
B. Bylsma, M. Carrigan, L.S. Durkin, C. Hill, M. Joyce, A. Lesauvage, M. Nunez Ornelas, K. Wei, B.L. Winer, B. R. Yates

Princeton University, Princeton, New Jersey, U.S.A.
F.M. Addesa, H. Bouchamaoui, P. Das, G. Dezoort, P. Elmer, A. Frankenthal, B. Greenberg, N. Haubrich, S. Higginbotham, G. Kopp, S. Kwan, D. Lange, A. Loeliger, D. Marlow, I. Ojalvo, J. Olsen, D. Stickland, C. Tully

University of Puerto Rico, Mayaguez, Puerto Rico, U.S.A.
S. Malik

Purdue University, West Lafayette, Indiana, U.S.A.
A.S. Bakshi, V.E. Barnes, S. Chandra, R. Chawla, S. Das, A. Gu, L. Gutay, M. Jones, A.W. Jung, D. Kondratyev, A.M. Koshy, M. Liu, G. Negro, N. Neumeister, G. Paspalaki, S. Piperov, A. Purohit, J.F. Schulte, M. Stojanovic[15], J. Thieman, F. Wang, W. Xie

Purdue University Northwest, Hammond, Indiana, U.S.A.
J. Dolen, N. Parashar, A. Pathak

JHEP01(2025)011

Rice University, Houston, Texas, U.S.A.
D. Acosta, A. Baty, T. Carnahan, S. Dildick, K.M. Ecklund, P.J. Fernández Manteca, S. Freed, P. Gardner, F.J.M. Geurts, A. Kumar, W. Li, O. Miguel Colin, B.P. Padley, R. Redjimi, J. Rotter, S. Yang, E. Yigitbasi, Y. Zhang

University of Rochester, Rochester, New York, U.S.A.
A. Bodek, P. de Barbaro, R. Demina, J.L. Dulemba, C. Fallon, A. Garcia-Bellido, O. Hindrichs, A. Khukhunaishvili, P. Parygin, E. Popova, R. Taus, G.P. Van Onsem

The Rockefeller University, New York, New York, U.S.A.
K. Goulianos

Rutgers, The State University of New Jersey, Piscataway, New Jersey, U.S.A.
B. Chiarito, J.P. Chou, Y. Gershtein, E. Halkiadakis, A. Hart, M. Heindl, D. Jaroslawski, O. Karacheban[25], I. Laflotte, A. Lath, R. Montalvo, K. Nash, M. Osherson, H. Routray, S. Salur, S. Schnetzer, S. Somalwar, R. Stone, S.A. Thayil, S. Thomas, J. Vora, H. Wang

University of Tennessee, Knoxville, Tennessee, U.S.A.
H. Acharya, A.G. Delannoy, S. Fiorendi, T. Holmes, N. Karunarathna, L. Lee, E. Nibigira, S. Spanier

Texas A&M University, College Station, Texas, U.S.A.
M. Ahmad, O. Bouhali[92], M. Dalchenko, A. Delgado, R. Eusebi, J. Gilmore, T. Huang, T. Kamon[93], H. Kim, S. Luo, S. Malhotra, R. Mueller, D. Overton, D. Rathjens, A. Safonov

Texas Tech University, Lubbock, Texas, U.S.A.
N. Akchurin, J. Damgov, V. Hegde, K. Lamichhane, S.W. Lee, T. Mengke, S. Muthumuni, T. Peltola, I. Volobouev, A. Whitbeck

Vanderbilt University, Nashville, Tennessee, U.S.A.
E. Appelt, S. Greene, A. Gurrola, W. Johns, R. Kunnawalkam Elayavalli, A. Melo, F. Romeo, P. Sheldon, S. Tuo, J. Velkovska, J. Viinikainen

University of Virginia, Charlottesville, Virginia, U.S.A.
B. Cardwell, B. Cox, J. Hakala, R. Hirosky, A. Ledovskoy, A. Li, C. Neu, C.E. Perez Lara

Wayne State University, Detroit, Michigan, U.S.A.
P.E. Karchin

University of Wisconsin — Madison, Madison, Wisconsin, U.S.A.
A. Aravind, S. Banerjee, K. Black, T. Bose, S. Dasu, I. De Bruyn, P. Everaerts, C. Galloni, H. He, M. Herndon, A. Herve, C.K. Koraka, A. Lanaro, R. Loveless, J. Madhusudanan Sreekala, A. Mallampalli, A. Mohammadi, S. Mondal, G. Parida,

JHEP01(2025)011

D. Pinna, A. Savin, V. Shang, V. Sharma, W.H. Smith, D. Teague, H.F. Tsoi, W. Vetens, A. Warden

Authors affiliated with an institute or an international laboratory covered by a cooperation agreement with CERN

S. Afanasiev, V. Andreev, Yu. Andreev, T. Aushev, M. Azarkin, A. Babaev, A. Belyaev, V. Blinov[94], E. Boos, V. Borshch, D. Budkouski, M. Chadeeva[94], V. Chekhovsky, M. Danilov[94], A. Dermenev, T. Dimova[94], D. Druzhkin[95], M. Dubinin[85], L. Dudko, A. Ershov, G. Gavrilov, V. Gavrilov, S. Gninenko, V. Golovtcov, N. Golubev, I. Golutvin, I. Gorbunov, Y. Ivanov, V. Kachanov, L. Kardapoltsev[94], V. Karjavine, A. Karneyeu, V. Kim[94], M. Kirakosyan, D. Kirpichnikov, M. Kirsanov, V. Klyukhin, O. Kodolova[96], D. Konstantinov, V. Korenkov, A. Kozyrev[94], N. Krasnikov, A. Lanev, P. Levchenko[97], O. Lukina, N. Lychkovskaya, V. Makarenko, A. Malakhov, V. Matveev[94], V. Murzin, A. Nikitenko[98,96], S. Obraztsov, V. Oreshkin, A. Oskin, V. Palichik, V. Perelygin, S. Petrushanko, V. Popov, O. Radchenko[94], V. Rusinov, M. Savina, V. Savrin, D. Selivanova, V. Shalaev, S. Shmatov, S. Shulha, Y. Skovpen[94], S. Slabospitskii, V. Smirnov, A. Snigirev, D. Sosnov, V. Sulimov, E. Tcherniaev, A. Terkulov, O. Teryaev, I. Tlisova, A. Toropin, L. Uvarov, A. Uzunian, A. Vorobyev[†], N. Voytishin, B.S. Yuldashev[99], A. Zarubin, I. Zhizhin, A. Zhokin

[†] *Deceased*
[1] *Also at Yerevan State University, Yerevan, Armenia*
[2] *Also at TU Wien, Vienna, Austria*
[3] *Also at Institute of Basic and Applied Sciences, Faculty of Engineering, Arab Academy for Science, Technology and Maritime Transport, Alexandria, Egypt*
[4] *Also at Université Libre de Bruxelles, Bruxelles, Belgium*
[5] *Also at Universidade Estadual de Campinas, Campinas, Brazil*
[6] *Also at Federal University of Rio Grande do Sul, Porto Alegre, Brazil*
[7] *Also at UFMS, Nova Andradina, Brazil*
[8] *Also at University of Chinese Academy of Sciences, Beijing, China*
[9] *Also at Nanjing Normal University, Nanjing, China*
[10] *Now at The University of Iowa, Iowa City, Iowa, U.S.A.*
[11] *Also at University of Chinese Academy of Sciences, Beijing, China*
[12] *Also at an institute or an international laboratory covered by a cooperation agreement with CERN*
[13] *Now at British University in Egypt, Cairo, Egypt*
[14] *Now at Cairo University, Cairo, Egypt*
[15] *Also at Purdue University, West Lafayette, Indiana, U.S.A.*
[16] *Also at Université de Haute Alsace, Mulhouse, France*
[17] *Also at Department of Physics, Tsinghua University, Beijing, China*
[18] *Also at Tbilisi State University, Tbilisi, Georgia*
[19] *Also at The University of the State of Amazonas, Manaus, Brazil*
[20] *Also at Erzincan Binali Yildirim University, Erzincan, Turkey*
[21] *Also at University of Hamburg, Hamburg, Germany*
[22] *Also at RWTH Aachen University, III. Physikalisches Institut A, Aachen, Germany*
[23] *Also at Isfahan University of Technology, Isfahan, Iran*
[24] *Also at Bergische University Wuppertal (BUW), Wuppertal, Germany*
[25] *Also at Brandenburg University of Technology, Cottbus, Germany*
[26] *Also at Forschungszentrum Jülich, Juelich, Germany*

JHEP01(2025)011

[27] *Also at CERN, European Organization for Nuclear Research, Geneva, Switzerland*
[28] *Also at Institute of Physics, University of Debrecen, Debrecen, Hungary*
[29] *Also at Institute of Nuclear Research ATOMKI, Debrecen, Hungary*
[30] *Now at Universitatea Babes-Bolyai — Facultatea de Fizica, Cluj-Napoca, Romania*
[31] *Also at Physics Department, Faculty of Science, Assiut University, Assiut, Egypt*
[32] *Also at HUN-REN Wigner Research Centre for Physics, Budapest, Hungary*
[33] *Also at Faculty of Informatics, University of Debrecen, Debrecen, Hungary*
[34] *Also at Punjab Agricultural University, Ludhiana, India*
[35] *Also at UPES — University of Petroleum and Energy Studies, Dehradun, India*
[36] *Also at University of Visva-Bharati, Santiniketan, India*
[37] *Also at University of Hyderabad, Hyderabad, India*
[38] *Also at Indian Institute of Science (IISc), Bangalore, India*
[39] *Also at IIT Bhubaneswar, Bhubaneswar, India*
[40] *Also at Institute of Physics, Bhubaneswar, India*
[41] *Also at Deutsches Elektronen-Synchrotron, Hamburg, Germany*
[42] *Now at Department of Physics, Isfahan University of Technology, Isfahan, Iran*
[43] *Also at Sharif University of Technology, Tehran, Iran*
[44] *Also at Department of Physics, University of Science and Technology of Mazandaran, Behshahr, Iran*
[45] *Also at Helwan University, Cairo, Egypt*
[46] *Also at Italian National Agency for New Technologies, Energy and Sustainable Economic Development, Bologna, Italy*
[47] *Also at Centro Siciliano di Fisica Nucleare e di Struttura Della Materia, Catania, Italy*
[48] *Also at Università degli Studi Guglielmo Marconi, Roma, Italy*
[49] *Also at Scuola Superiore Meridionale, Università di Napoli 'Federico II', Napoli, Italy*
[50] *Also at Fermi National Accelerator Laboratory, Batavia, Illinois, U.S.A.*
[51] *Also at Università di Napoli 'Federico II', Napoli, Italy*
[52] *Also at Ain Shams University, Cairo, Egypt*
[53] *Also at Consiglio Nazionale delle Ricerche — Istituto Officina dei Materiali, Perugia, Italy*
[54] *Also at IRFU, CEA, Université Paris-Saclay, Gif-sur-Yvette, France*
[55] *Also at Riga Technical University, Riga, Latvia*
[56] *Also at Department of Applied Physics, Faculty of Science and Technology, Universiti Kebangsaan Malaysia, Bangi, Malaysia*
[57] *Also at Consejo Nacional de Ciencia y Tecnología, Mexico City, Mexico*
[58] *Also at Trincomalee Campus, Eastern University, Sri Lanka, Nilaveli, Sri Lanka*
[59] *Also at INFN Sezione di Pavia, Università di Pavia, Pavia, Italy*
[60] *Also at National and Kapodistrian University of Athens, Athens, Greece*
[61] *Also at Ecole Polytechnique Fédérale Lausanne, Lausanne, Switzerland*
[62] *Also at Universität Zürich, Zurich, Switzerland*
[63] *Also at Stefan Meyer Institute for Subatomic Physics, Vienna, Austria*
[64] *Also at Laboratoire d'Annecy-le-Vieux de Physique des Particules, IN2P3-CNRS, Annecy-le-Vieux, France*
[65] *Also at Near East University, Research Center of Experimental Health Science, Mersin, Turkey*
[66] *Also at Konya Technical University, Konya, Turkey*
[67] *Also at Izmir Bakircay University, Izmir, Turkey*
[68] *Also at Adiyaman University, Adiyaman, Turkey*
[69] *Also at Necmettin Erbakan University, Konya, Turkey*
[70] *Also at Bozok Universitetesi Rektörlügü, Yozgat, Turkey*
[71] *Also at Marmara University, Istanbul, Turkey*
[72] *Also at Milli Savunma University, Istanbul, Turkey*
[73] *Also at Kafkas University, Kars, Turkey*
[74] *Also at Hacettepe University, Ankara, Turkey*
[75] *Also at Istanbul University — Cerrahpasa, Faculty of Engineering, Istanbul, Turkey*
[76] *Also at Ozyegin University, Istanbul, Turkey*
[77] *Also at Vrije Universiteit Brussel, Brussel, Belgium*

JHEP01(2025)011

[78] Also at School of Physics and Astronomy, University of Southampton, Southampton, United Kingdom
[79] Also at University of Bristol, Bristol, United Kingdom
[80] Also at IPPP Durham University, Durham, United Kingdom
[81] Also at Monash University, Faculty of Science, Clayton, Australia
[82] Also at Università di Torino, Torino, Italy
[83] Also at Bethel University, St. Paul, Minnesota, U.S.A.
[84] Also at Karamanoğlu Mehmetbey University, Karaman, Turkey
[85] Also at California Institute of Technology, Pasadena, California, U.S.A.
[86] Also at United States Naval Academy, Annapolis, Maryland, U.S.A.
[87] Also at Bingol University, Bingol, Turkey
[88] Also at Georgian Technical University, Tbilisi, Georgia
[89] Also at Sinop University, Sinop, Turkey
[90] Also at Erciyes University, Kayseri, Turkey
[91] Also at Horia Hulubei National Institute of Physics and Nuclear Engineering (IFIN-HH), Bucharest, Romania
[92] Also at Texas A&M University at Qatar, Doha, Qatar
[93] Also at Kyungpook National University, Daegu, Korea
[94] Also at another institute or international laboratory covered by a cooperation agreement with CERN
[95] Also at Universiteit Antwerpen, Antwerpen, Belgium
[96] Also at Yerevan Physics Institute, Yerevan, Armenia
[97] Also at Northeastern University, Boston, Massachusetts, U.S.A.
[98] Also at Imperial College, London, United Kingdom
[99] Also at Institute of Nuclear Physics of the Uzbekistan Academy of Sciences, Tashkent, Uzbekistan

JHEP01(2025)011